7

Nanomaterials and Biocompatibility: BioMEMS and Dendrimers

Sean T. Zuckerman and Weiyuan John Kao

Introduction

"Biocompatibility" is a term often used by researchers and laypersons. The website for the National Institutes of Health uses the word biocompatibility more than 300 times (www.nih.gov); yet a clear definition of biocompatibility is difficult to locate. What criteria define biocompatibility? Scientists have struggled to define the word biomaterial. Therefore it follows there has been much difficulty quantifying biocompatibility. The European Society for Biomaterials called a consensus conference in 1986 to define basic terms such as biomaterial, host response, and biocompatibility. The attending members agreed that biocompatibility is, "the ability of a material to perform with an appropriate host response in a specific application." The host response was subsequently defined as, "the reaction of a living system to the presence of a material" (Williams, 1987). This definition of biocompatibility begs the question, "What is an 'appropriate' host response?" To determine what is an "appropriate" host response requires measurement of a biological phenomenon. Both the extent and the duration of the host response are critical factors determining the appropriateness of the body's response. The difficulty therefore lies in quantifying a graded response. In vitro tests enable more comprehensive and invasive analysis but are limited in scope to simplified models. In vivo testing, on the other hand, offers more physiologically relevant data but is not always feasible or ethical to perform. In addition, in vivo testing is complicated by complex interactions between multiple systems. Therefore a combination of in vitro and in vivo testing must be performed to draw relevant and accurate conclusions.

In order to provide uniformity and guidance, the International Organization for Standardization (ISO) (www.iso.org, 2003) and the American Society for Testing Materials Standards have constructed guidelines to aid industry and academic researchers. Table 7.1 shows the breakdown of ISO 10993. Part 1 outlines the basis for evaluating medical devices including classifying the device based on the type and length of contact with the host. Part 1 then outlines the appropriate tests necessary to analyze interactions

M.M. de Villiers et al. (eds.), *Nanotechnology in Drug Delivery*, DOI: 10.1007/978-0-387-77667-5_7,

Table 7.1. International organization for standardization 10993 biological evaluation of medical devices (ISO, 2006).

Part	Title
1	Evaluation and testing within a risk management system
2	Animal welfare requirements
3	Tests for genotoxicity, carcinogenicity, and reproductive toxicity
4	Selection of tests for interactions with blood
5	Tests for in vitro cytotoxicity
6	Tests for local effects after implantation
7	Ethylene oxide sterilization residuals
9	Framework for identification and quantification of potential degradation products
10	Tests for irritation and delayed-type hypersensitivity
11	Tests for systemic toxicity
12	Sample preparation and reference materials
13	Identification and quantification of degradation products from polymeric medical devices
14	Identification and quantification of degradation products from ceramics
15	Identification and quantification of degradation products from metals and alloys
16	Toxicokinetic study design for degradation products and leachables
17	Establishment of allowable limits for leachable substances
18	Chemical characterization of materials
19	Physico-chemical, morphological, and topographical characterization of materials
20	Priniciples and methods for immunotoxicology testing of medical devices

with the body based on the class of material. The remaining 18 subsections to ISO 10993 cover a range of tests to determine blood compatibility (ISO 10993-4), in vitro cytotoxicity (ISO 10993-5), local (ISO 10993-6) and systemic (ISO 10993-11) effects post-implantation, identification of degradation products (ISO 10993-13, -14, and -15), as well as material characterization (ISO 10993-18 and -19). The American Society for Testing Materials Standards has similar protocols outlined under F748 Standard practice for selecting generic biological test methods for materials and devices. This F748 protocol also addresses pyrogen testing as well as batch testing for production lots (American Society for Testing Materials Standards, 2004). The Food and Drug Administration issued a blue book memorandum (G95-1) in May of 1995 based on the ISO 10993 Biological Evaluation of Medical Devices document governing approval of medical devices for commercial sale in the United States of America (United States Food and Drug Administration, 1995). This blue book document adopted the material categories from ISO 10993 and instituted additional testing requirements. The American Society for Testing Materials Standards F748, ISO 10993, and G95-1 therefore establish the minimum body of knowledge necessary for commercialization of medical devices.

The two chapters on "Biocompatibility of Nanotechnology" will focus on the biocompatibility of current and emerging nanomaterials such as bioMEMS, dendrimers, carbon nantotubes, and fullerenes from a

structure–function standpoint. Liposomes have been researched since the late 1970 s and their toxicity and compatibility are relatively well characterized. Hence liposomes will not be discussed. Several reviews have been published on the matter (Zhang, Liu & Huang, 2005; Vermette & Meagher, 2003; Lian & Ho, 2001; Woodle & Scaria, 2001; Kaneda, 2000; Nagayasu, Uchiyama, & Kiwada, 1999). We will present trends and data from current primary literature correlating the structure of a material with its observed effect on the body ranging from cytotoxicity to hypersensitivity. In addition, we will highlight the differences in the data obtained ranging from different material preparation methods to different animal models and how these upstream choices influence the comparison of conclusions drawn regarding each type of material. The subjective nature of assessing the extent of a biological phenomenon such as the host response to a given material for a species should become apparent.

Known Structure–Function Relationships

BioMEMS and Nanobiotechnology

The field of nanobiotechnology has been growing rapidly over the past decade. Advances in micro- and nanofabrication technologies have spurred much of the growth (Blattler, Huwiler, Ochsner, Stadler, Solak, Voros, & Grandin, 2006). Nanobiotechnology involves materials and molecules less than 100 nm in size while the microelectro-mechanical systems (MEMS) are designed to function on the micrometer scale. However, the two have become tightly entwined recently as research into biosensors and drug delivery vehicles increases (Gourley, 2005). Biological MEMS (bioMEMS) are designed to interact with a biological environment either as a sensor or directly through drug delivery or electrical stimulation (Meyer, 2002). The recent advances in nanofabrication technology have enabled increased potential for diagnostic capabilities through the ability to pattern biological molecules such as enzymes onto a given substrate. BioMEMS interface with nanobiotechnology by providing the substrate and microscale architecture to direct fluid to the biological molecules as shown in Figure 7.1. In addition, bioMEMS provide the ability to take mechanical or electrical action based on the output from the nanoscale analysis. This coupling has led to the development of glucose sensors using enzymatic detection of glucose levels that could be followed by insulin release stimulated by the bioMEMS (Figure 7.1) (Zimmerman, Fienbork, Flounders, & Liepmann, 2004).

Implantable microscale sensors have been identified as a market estimated to surpass $10 billion USD by 2008 (Gourley, 2005). BioMEMS are ideal candidates for these implantable sensors because they couple the ability to analyze complex solutions such as those found in vivo with actuating the appropriate response in an implantable format. In addition, nanoarrays of biological molecules such as enzymes on bioMEMS could perform diagnostic analysis in vivo aiding diagnosis of the patient's condition by medical staff. BioMEMS are also capable of recording force transduction in heart muscle (Lin, Pister, & Roos, 2000) and integrating

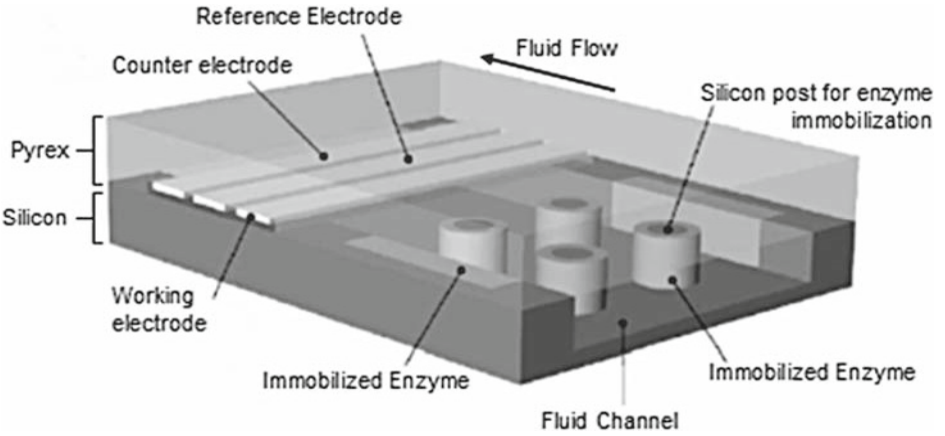

Figure 7.1 An example of a bioMEMS-based sensor. Adapted from Zimmerman et al. (2004).

neurological functions such as retinal implants to restore lost vision (Meyer, 2002). The ability to integrate molecular motors into bioMEMS also exists (Hiratsuka, Miyata, Tada, & Uyeda, 2006). Microfluidic bioMEMS offer researchers the ability to carefully manipulate cell conditions at the level of individual cells (Chin, Taupin, Sanga, Scheel, Gage, & Bhatia, 2004). Researchers have constructed microfluidic devices to control biochemical signals allowing a complex matrix of conditions to be analyzed on one device simultaneously (Ziaie, Baldi, Lei, Gu, & Siegel, 2004). This multitude of conditions enables researchers to determine the gradient effect of different growth factors or cytokines upon stem cell differentiation ex vivo, for instance.

The tremendous potential for bioMEMS to address many problems currently plaguing researchers has led the field to focus on functionality and manufacturing capabilities. However, an implantable device must be tolerated and integrated into the host for long-term efficacy. Little research has been done investigating the biocompatibility of bioMEMS. Even less research has been performed to determine the effect that sterilization and packaging have upon biocompatibility. Madou (1997) addressed the need for more attention to compatibility issues nearly 10 years ago. "Biocompatibility is the single most complex factor facing in vivo sensor development and it needs addressing up front in the sensor design." This information vacuum can be partly explained by previous medical applications of MEMS. Many devices such as pacemakers are entirely encapsulated within a sealed vessel such as a titanium (Ti) shell. Therefore only the compatibility of the Ti shell and the exposed lead insulator are required for implantation (Kotzar, Freas, Abel, Fleischman, Roy, Zorman, Moran, & Melzak, 2002). In the past researchers have relied on previous biocompatibility testing of similar materials. The difficulty in relying on these previous studies is that many of them investigated the compatibility of a particular material for applications experiencing different mechanical and cellular environments. For instance, data from silicon carbide (SiC)-coated stents (Amon, Bolz, & Schaldach, 1996) or orthopedic joints (Nordsletten, Hogasen, Konttinen, Santavirta, Aspenberg, &

Aasen, 1996) has been used to gauge the compatibility of SiC for bioMEMS applications. The ISO and FDA have standards for sterilization of medical devices for implantation (ISO 10993 and G95-1). Many of the previous studies either have not conformed to established sterilization procedures or did not specify how sterilization was achieved. The ISO 10993 guidelines represent the minimum knowledge needed to commercialize a given device or material. In many cases the tests recommended by ISO 10993 must be expanded in scope or depth or supplemented with additional testing to obtain a full characterization of compatibility. BioMEMS and nanobiotechnology are difficult to isolate and will thus be discussed herein simultaneously. The survey presented here focuses mainly on bioMEMS compatibility but applies to bioMEMS with nanopatterning and immobilized biological molecules as well.

Non-ISO 10993 Biocompatibility Testing

Silicon-Based Materials

Silicon is used extensively in integrated circuits and has been adopted as a substrate for many MEMS because the processing is well characterized and enables electrical conduction (Stoldt & Bright, 2006; Zhu, Zhang, & Zhu, 2005). Previously nanocrystals of silicon have been shown in a number of studies to exhibit no significant cytotoxicity (Bayliss & Buckberry, 1999; Bayliss, Heald, Fletcher, & Buckberry, 1999; Bayliss, Harris, Buckberry, & Rousseau, 1997; Bayliss, Buckberry, Harris, & Tobin, 2000). While Bayliss and Buckberry's research found no significant toxicity, Kubo and co-workers (1997) observed nodule formation by periodontal ligament fibroblasts in response to what they hypothesized was silicon leaching from glass. Ten nanometer pores were found to be the optimal substrate for B50 neuronal growth compared to bulk polished silicon or plasma-enhanced chemical vapor deposition. However, Chinese hamster ovary cells demonstrated affinity for the plasma-enhanced chemical vapor-deposited silicon over the polished or nanoporous silicon surfaces showing a cell-type-dependent relationship between cell viability and surface architecture (Bayliss & Buckberry 1999). Bayliss et al. (2000) also investigated sterilization procedures and determined that autoclaving was optimal.

Research on another silicon-based material, silicon carbide (SiC), found that the α form was marginally more cytotoxic than the β form at doses above 0.1 mg/ml to macrophages, osteoblast-like cells, and fibroblasts (Allen, Butter, Chandra, Lettington, & Rushton, 1995). Radiofrequency sputtering of SiC did not appear cytotoxic; however, attachment of fibroblasts and osteoblasts was lower than desired and proliferation of osteoblasts was inhibited (Naji & Harmand, 1991). Amon et al. (1996) followed ISO 10993-5 guidelines for cytotoxicity experiments testing L929 murine fibroblasts' response to SiC-coated tantalum stents. The SiC coating showed no cytotoxicity or mutagenicity in these experiments, but the applicability of SiC-coated stents to bioMEMS is limited. Stents need to withstand high shear stress induced from fluid flow and are in intimate contact with blood, which some bioMEMS may not experience, in vivo.

In addition to SiC, silicon nitride (Si_3N_4) nanopowder has also been investigated for compatibility in vitro and in vivo. Rabbit marrow stromal

cells were initially adhered to the upper surface of Si_3N_4 disks but spread to only the edges after 4 weeks (Wan, Williams, Doherty, & Williams,1994). Marrow stromal cells cultured with Si_3N_4 and implanted for 5 weeks showed differentiation around the Si_3N_4 but not on the surface or within the pores. Interestingly, porous bone was observed to integrate with the Si_3N_4 when the Si_3N_4 was directly implanted into the femoral marrow cavity. In other in vitro testing, the human osteosarcoma MG-63 cell line showed no decrease in DNA synthesis after incubation with 1, 10, or 100 μg/ml Si_3N_4 nanoparticles for 48 h compared to the polystyrene-negative control (Sohrabi, Holland, Kue, Nagle, Hungerford, & Frondoza, 2000). Reaction-bonded silicon nitride disks showed an increase in the pro-inflammatory cytokines interleukin 1β or tumor necrosis factor alpha and sintered-reaction-bonded silicon nitride showed no change in these cytokines compared to the negative control surface. Kue and colleagues (1999) came to a similar conclusion that the sintering process resulted in little change in MG-63 cell proliferation and metabolism. These experiments revealed that material processing can have a significant effect upon downstream cellular responses even though the mechanistic impact of sintering on MG-63 cells was not elucidated.

In addition to cell adhesion, the hemocompatibility is a critical factor determining the efficacy of blood-contacting devices. The hemocompatibility of various materials commonly used in MEMS was measured as a function of platelet adhesion (Weisenberg & Mooradian, 2002). Platelets were isolated from human donors and cultured statically for 5 min at which time the platelets were imaged and counted. Si, Si_3N_4, low-stress silicon nitride ($S_{1.0}N_{1.1}$), and SU-8 photoresist all exhibited higher platelet adhesion than the Chronoflex AR/LT polycarbonate (PC) -based polyurethane control. These materials are all common bioMEMS components and therefore relevant. Platelet adhesion to SiO_2 and thin parylene C films were not significantly different from the control surface. The PC-based polyurethane was chosen based on previous literature demonstrating its hemocompatibility (Elam & Nygren, 1992; Chen, Zhang, Kodama, & Nakaya, 1999); however, the data based on spreading and circularity obtained indicated the choice of reference material may not be appropriate (Weisenberg & Mooradian, 2002).

Many implantable bioMEMS will have intimate contact with blood such as biosensors for glucose. The hemocompatibility is critical to the efficacy of such blood-contacting devices as well as cellular compatibility since many types of cells circulate in the blood. Thus various SiN_x:H films created by plasma-enhanced chemical vapor deposition were tested for hemocompatibility with platelets (Wan, Yang, Shi, Wong, Zhou, Huang, & Chu, 2005). The number of N atoms was varied to change the degree of hydrophilicity. The samples were incubated with human platelets for 2 h and the results compared against low-temperature isotropic pyrolytic carbon, which is the most commonly used material in commercialized medical devices contacting blood (Wan et al., 2005). Platelets were chosen based on their role in coagulation and thrombus formation, which can have serious implications if a blood-contacting device tips the homeostatic equilibrium in the blood. Wan et al. (2005) found that platelets adhered less to the three forms of SiN_x:H than to the low-temperature

isotropic pyrolytic carbon. Scanning electron microscopy analysis showed less pseudopodia and spreading, which has been shown to be indicative of thrombus formation (Gibbins, 2004). Wan et al. (2005) hypothesized that the hydrophilic nature of the surface induced less conformational rearrangement in the proteins adsorbed to the surface resulting in lower protein adhesion and less platelet activation. Surprisingly no hemolysis of red blood cells was investigated. Little other hemocompatibility data is published for any material used in MEMS devices thus the applicability of this data is rather limited. In addition, most devices considered for implant will have much more complex architecture than simple plasma-enhanced chemical vapor deposition coatings limiting these findings further. More extensive characterization of commonly used MEMS materials following ISO 10993 needs to be published to help guide researchers in material selection during the design phase.

Implantation in sub-cutaneous cages was used to determine the inflammatory response of Sprague–Dawley rats to silicon-based microreservoir MEMS (Voskerician, Shive, Shawgo, von Recum, Anderson, Cima, & Langer, 2003). The components of the microreservoir drug delivery MEMS tested were: Si, Si_3N_4, SiO_2, gold, and Su-8. The leukocyte concentration in the exudate was determined as was the number of adherent macrophages and foreign body giant cells, which was used as a determinant of protein adsorption. With the exception of Si, all of the exudate from materials tested at 7 and 14 days showed similar leukocyte concentrations as the empty cage implant indicating minimal acute and chronic inflammation resulting from the material residing within the cage. The leukocyte concentration in the Si-containing cage tapered off after 21 days but was still higher than the negative control levels. SU-8 was found to exhibit delamination after 21 days; SiO_2 and Si_3N_4 showed similar biofouling levels inferred from macrophage and foreign body giant cell numbers leaving the choice for dielectric layer to be determined by mechanical demands and/or fabrication limitations (Voskerician et al., 2003). This data is an important step to characterizing the in vivo response to bio-MEMS components.

Nanostructured Titanium (Ti)

Nanostructured TiO_2 has been investigated for its role as a cellular adhesive substrate. Mouse fibroblasts showed enhanced adhesion to porous TiO_2 with 50–200 nm diameter pores that were 25–75 nm deep (Zuruzi, Butler, MacDonald, & Safinya, 2006). The fibroblasts adhered to the porous TiO_2 more rapidly than SiO_2 or Si_3N_4 up to 18 hr; after 24 h adhesion was not significantly different for the three materials. Scanning electron microscopy analysis of cell morphology revealed more spherical cells on SiO_2 than nanoporous TiO_2 indicating less adhesion and less interaction. Interestingly, the fibroblasts adhered to and adopted the shape of square micropatterned nanoporous TiO_2 structures 10 and 20 μm long. However, Webster and co-workers (2000) found that fibroblasts adhered less to nanoporous alumina (Al_2O_3), titania (TiO_2), and hydroxyapatite ($Ca_5(PO_4)_3(OH)$) than the traditional ceramics after 4 h. Endothelial cells exhibited similar behavior to fibroblasts. Osteoblasts conversely showed more adhesion to these nanoporous ceramics than the

conventional forms. This increased osteoblast adhesion was attributed to increased vitronectin adsorption on the nanoporous ceramics (Webster et al., 2000).

Surface Modification of Various Substrates:* In Vitro *Assessment

As Voskerician et al. (2003) noted biofouling is an important phenomenon for all implanted devices including bioMEMS. Cells interact with implanted materials through a layer of adsorbed proteins. Many researchers believe that eliminating protein adsorption will eliminate the current problems of fibrous capsule formation, sustained chronic inflammation, and material degradation. Surface modification is one popular technique to decrease protein adsorption and thus biofouling. In particular the use of polyethylene glycol (PEG) (Figure 7.2) has been adopted to minimize or direct protein adsorption depending upon the application. For bioMEMS applications the PEG film thickness varies between 2 and 20 nm and exhibits a hydrophilic character resulting from the PEG-modified surface and not the underlying substrate (Richards Grayson, Shawgo, Johnson, Flynn, Li, Cima, & Langer, 2004). Sharma and colleagues (2002) modified silicon surfaces with PEG using two different methods: solution phase PEG–silane coupling or vapor deposition of polyethylene oxide. The PEG–silane solution chemistry allowed for the addition of 2 nm of PEG. The low nanometer thickness of the PEG film is crucial for efficacy of biosensor MEMS that require diffusion to and from the material. Both vapor deposition and solution coupling yielded similar decreases in fibrinogen and bovine serum albumin adsorption, which represent a range of protein molecular weights that many bioMEMS will encounter in vivo. Lee, Bhushan, & Hansford (2005) found similar results using vapor deposition to deposit two fluoropolymers or fluorosilane on silicon wafers. This method yielded film thicknesses <10 nm for all three polymers with fluorosilane exhibiting characteristics of a monolayer. Thus vapor deposition is an attractive surface modification technique for multiple polymers allowing researchers to tailor hydrophobicity/hydrophilicity with surface thickness and roughness in order to optimize the coating for the various nanoscale architectures of the device such as fluid channels or micro/nanoreservoirs. Hanein, Pan, Ratner, Denton, & Bohringer (2001) achieved similar results using photolithography to produce PEG films. PEG modification via photolithography or vapor deposition allows for precise control of PEG modification and thus preserves the electrical conductivity compared to the solution phase chemistry, which offers no control over surface modification patterns. Thus solution phase PEG modification could modify electrical leads or plug channels within the device reducing or eliminating its function. Therefore as the complexity of bioMEMS increases, the use of solution phase surface modification will likely decrease significantly. PEG

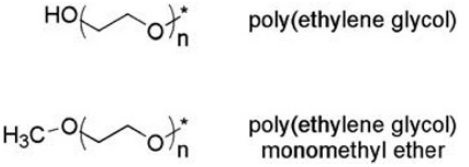

Figure 7.2 Poly(ethylene glycol) and monomethyl ether poly(ethylene glycol) are used for modification of various surfaces to minimize protein adsorption.

surface modification was used to create hydrophilic channels in a microfluidic network based on Si, gold, or polydimethylsiloxane (Papra, Bernard, Juncker, Larsen, Michel, & Delamarche, 2001). The PEG chains prevent protein adsorption to the fluidic channels while creating a hydrophilic environment that allows proteins to diffuse along the microfluidic channel and deposit into patterned microreservoirs. Si–PEG–Si was identified as the best choice for modification of polydimethylsiloxane leading to hydrophilic stability for up to 3 weeks (Papra et al., 2001). Gold MEMS surfaces are very flexible allowing researchers to selectively pattern one alkanethiol via microcontact printing and masking the remaining gold surface with a second alkanethiol in solution. Thus complex patterns can be created leading to selective protein adsorption or the creation of complex fluidic channels leading to microreservoirs.

Chemical vapor deposition of various forms of poly(*p*-xylenes) has also been shown to successfully modify enclosed, complex microchannels on silicon using polydimethylsiloxane molds (Chen, Elkasabi, & Lahann, 2005). The channels were open on both ends and ranged from 1600 μm for a straight channel to 2800 μm for an S-curved channel. This meandering channel formed a series of S-curves with an aspect ratio of 37; the straight channel had an aspect ratio of 21. The film thickness varied by xylene isoform deposited but was homogeneous throughout the film for each polymer, which is difficult to achieve through other surface modification methodologies for materials with high aspect ratios. Xylene also retained its functionality after chemical vapor deposition as evidenced by biotin conjugation and visualization via rhodamine (Chen et al., 2005). Thus chemical vapor deposition has shown uniform modification of simple and complex surfaces providing researchers a powerful tool to modify complex micro and nanoscale patterning on bioMEMS.

In addition to PEG, other polymers have been investigated for their non-fouling properties and cytotoxicity. Silica gels were investigated as a potential surface coating to prevent the undesired adsorption of proteins to glucose sensors (Kros, Gerritsen, Sprakel, Sommerdijk, Jansen, & Nolte, 2001). Tetraethylorthosilicate was mixed with PEG, heparin, dextran sulfate, Nafion, or polystyrene sulfonate to form sol gel, which is a soluble colloidal suspension that can be gelled into a workable solid. While the sol gel-based coatings showed similar hydrophilicity, human dermal fibroblasts adhered to and proliferated on sol gel, sol gel-heparin, sol gel-Nafion, and sol gel-PEG at the same level as the Thermanox coverslip used as a negative control (Kros et al., 2001). The level of fibroblast adhesion and proliferation on sol gel-polystyrene sulfonate and sol gel-dextran sulfate was much lower than the reference surface. However, the morphology of the fibroblasts on the sol gel-polystyrene sulfonate and sol gel-dextran sulfate surfaces was normal indicating that cell adhesion was lower rather than surface-mediated toxicity. Because both polystyrene sulfonate and dextran sulfate have a high number of sulfate groups available for cellular interactions, Kros et al. (2001) hypothesized that the sulfate groups mediate fibroblast adhesion and proliferation. In vitro testing of the coated glucose sensor also revealed that the sol gel-coated glucose sensors retained more activity than uncoated sensors in complete serum while maintaining the same level of activity in an albumin solution. Thus

various additives to silica gel are successful in mediating adsorption of serum proteins while retaining non-toxic properties toward human dermal fibroblasts. This coating could therefore be used to help increase the compatibility and function of an implanted bioMEMS into the host tissue while retaining activity.

Photolithography can also be used to create self-assembling monolayers on the MEMS surface maintaining any surface-dependent functionality (Richards Grayson et al., 2004). Monolayers have been created from oligomers of ethylene oxide and PEG terminated with various end groups such as alkoxysilyl or trichlorosilyl. Self-assembled monolayers enable researchers to finely control both thickness and density of the surface modification. Tokachichu and Bhushan (2006) modified polymethylmethacrylate and polydimethylsiloxane with a perfluorodecyltriethoxysilane self-assembling monolayer. Protein adsorption to both surfaces was not significantly different as measured by atomic force microscopy using a fetal bovine serum-coated needle in phosphate-buffered saline solution or in air. This low level of protein adhesion could allow flow through nanoscale channels on microfluidic devices. Monomethyl ether PEG (mPEG) (Figure 7.2) modified silicon surfaces exhibited decreased fibrinogen and immunoglobulin G adsorption compared to non-modified clean silicon (Lan, Veiseh, & Zhang, 2005). Murine fibroblasts and macrophages on the mPEG-modified Si surfaces demonstrated lower adhesion correlating to lower protein adsorption. Fibroblasts showed similar morphology on both clean Si and mPEG-modified Si while macrophages exhibited a more round morphology on the mPEG-modified Si surface. When gold ridges or squares were patterned on the surface more protein adhered to the patterned gold areas of the surface than the mPEG-modified areas. Because little to no protein adsorbed onto the mPEG-modified Si the fibrinogen and immunoglobulin G showed concentrated adsorption on the gold patterns. Finally, cells were cultured on gold-patterned Si surfaces where the non-patterned portions of the Si were modified with mPEG to resist protein adsorption (Lan et al., 2005). Fibronectin was allowed to adsorb on to the modified Si surface followed by culture with fibroblasts or macrophages for 24 h. Both the macrophages and fibroblasts adhered only to the gold patterns and aligned with the topographical features of squares or ridges. Thus mPEG was shown to be an effective surface modification to direct protein adsorption and consequently cell adhesion onto Si surfaces patterned with gold. Self-assembled monolayers on bioMEMS have also been successfully created from phospholipid-based Langmuir–Blodgett films (Kim, Kim, & Byun, 2001). Therefore researchers can use various methods such as solution phase chemistry, lithography, or chemical vapor deposition to selectively modify bioMEMS surfaces to enhance functionality and efficacy.

Surface Modification of Various Substrates: In Vivo *Assessment*

A limited number of in vivo studies have been performed with surface-modified bioMEMS sensors. Ishikawa and colleagues (1998) found that glucose sensors with PEG-modified sensor tips functioned for 3 days in 20 patients with a sensitivity range of 2–28 mmol/L and a 10 min response time, which compared favorably to other sensors that reported response

times of 20–45 min. Another group reported glucose sensing activity 14 days post-implantation using a needle sensor modified with the phospholipid-based copolymer 2-methacryloyloxyethylphosphorylcholine and *n*-butylmethacrylate (Ishihara, Nakabayashi, Nishida, Sakakida, & Shichiri, 1994). The phospholipid nature of this surface modification is theorized to elicit similar interactions with proteins as host cells in vivo (Wisniewski & Reichert, 2000). This type of phospholipid polymeric surface modification has many difficulties to commercialization. Most importantly the coating can limit diffusion to the sensor immediately decreasing its efficacy. In addition, delamination from the sensor due to poor adhesion or mechanical stress is difficult to quantify (Wisniewski & Reichert, 2000). These polymeric surface modifications may also be detrimental to any biological molecules such as enzymes contained in the sensor. Various types of fluid flow systems have been developed to prevent protein adsorption and hence cell adhesion but will not be addressed here since these systems require constant perfusion and do not directly address the issue of biocompatibility (Wisniewski & Reichert, 2000). Other surface treatments such as the perfluorosulfonic acid polymer known as Nafion have been investigated based on their ease of application. Nafion can be dip coated onto sensors; however, this method does not allow for control over the surface pattern meaning microfluidic channels and other reservoir-like features can become clogged. Although Nafion did improve the immunogenicity and increased sensor functioning to 10 days post-implantation (Moussy, Harrison, & Rajotte, 1994). The in vivo trials conducted thus far have focused more on sustaining sensor activity than on solving long-term implantation issues. Researchers have used various surface coatings to resist protein adsorption and cell adhesion. To varying degrees the studies have worked but have not correlated directly to the compatibility between implanted materials and the host.

ISO 10993 Biocompatibility Testing

While the previous studies made relevant observations and important conclusions regarding material compatibility, few published studies adhered to the guidelines outlined by ISO 10993 for characterization of a biomaterial. One of the first papers to apply the ISO standard tests also investigated sterilization effects (Kotzar et al., 2002). The materials were chosen to cover a wide array of materials used in bioMEMS including Si-based materials, Ti, and SU-8 photoresist epoxy. The negative surface control was polyethylene per the United States Pharmacopeia's standard for implantation experiments. Both autoclaving and γ-irradiation were used to sterilize materials. The materials were characterized under the guidelines of ISO 10993-14 including extractables, infrared analysis, and mechanical testing. Scanning electron microscopy was also performed pre- and post-sterilization to determine any sterilization-dependent surface changes in the material. The scanning electron microscopy micrographs revealed no apparent damage to the material surface. However, Kotzar did note that the SU-8 surface was difficult to image because the surface is very smooth. The material extracts were classified as less than Grade 2 toward the L929 murine fibroblast line meaning the material can officially be

classified as "mildly reactive." This label satisfies the ISO 10993 criteria that the material extracts be less than a Grade 2 response and the positive control be a Grade 3 or 4. To further verify their in vitro findings, Kotzar et al. (2002) implanted these materials into rabbits for 1 or 12 weeks analyzing the results via histological staining. The fibrous capsule observed around the test materials was nearly "indistinguishable from the [polyethylene] negative controls." The in vivo data was important because the ASTM standard F67 outlines standards for commonly used Ti alloy processing methods for implantable Ti but does not cover Ti sputtering. The sputtered Ti surfaces tested by Kotzar et al. (2002) exhibited similar results to those previously obtained for sputtered Ti (Johansson, Hansson, & Albrektsson, 1990). Similarly, no established standards existed for SiC or Si_3N_4. Thus the preliminary results based on ISO 10993 testing by Kotzar et al. (2002) showed that SiC and Si_3N_4 prepared via standard MEMS processing techniques elicit no significant biological response. This conclusion is among the first direct data using established guidelines that supports the compatibility of these materials in MEMS applications.

Summary

An increased demand for implantable bioMEMS has surfaced in the past 5–10 years. Therefore in depth in vitro and in vivo biocompatibility testing is not yet widely performed. The extent of biocompatibility testing published investigates the components of bioMEMS rather than entire devices and does not follow the guidelines established by ISO 10993 for characterization of implantable materials. Therefore compatibility testing adhering to ISO 10993 standards needs to be performed on all components of bioMEMS. This biocompatibility data would then aid researchers during sensor design as predicted by Madou nearly a decade ago.

Dendrimers

Dendrimers exhibit low polydispersity and a reproducible pharmacokinetic profile making them ideal candidates for drug delivery (Yang & Kao, 2006; Boas & Heegaard, 2004). The functional groups (Figure 7.3) present on the dendrimer surface provide an easy mechanism to conjugate drug to

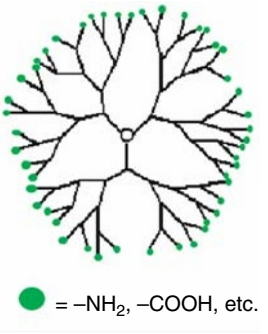

Figure 7.3 Dendrimer functional groups allow complexation or conjugation with various molecules such as DNA or pharmaceutical agents. (*See* Color Plate 13)

the surface in addition to physical encapsulation during dendrimer synthesis (Patri, Kukowska-Latallo, & Baker, Jr., 2005). However, their behavior in vivo is the most critical determinant of their efficacy. Myriad factors of dendrimer structure contribute to in vivo behavior including but not limited to: molecular weight, architecture, surface charge, and hydrophilicity/hydrophobicity. Therapeutic drug will be difficult to deliver to the desired target if the dendrimer is cleared rapidly from the bloodstream. Thus toxicity and blood clearance, or blood half-life, are potential roadblocks to the development of dendrimer-based drug delivery systems.

In vitro cytotoxicity is one of the first tests performed to characterize a potential candidate's in vivo toxicity. If the dendrimer proves to be excessively toxic to immortalized cell lines then the dendrimer will likely exhibit similar behavior in vivo. Additional testing such as hemolysis of red blood cells is performed to determine the effects of dendrimers in the bloodstream. Finally, radiolabeled dendrimer is used to determine in vivo distribution and blood clearance in animal models. Toxicity to vital organs such as the lungs, liver, or kidneys and ultimately morbidity may result if the dendrimer accumulates in these organs. Thus in vitro testing such as cytotoxicity and hemolysis combined with in vivo animal testing to determine preferential localization and excretion pathways of dendrimers provides a reasonable model to support or reject testing in humans. The structure–function relationship of dendrimer-induced biological response in different cell and animal models is highlighted. A brief summary of the experiments reviewed here is shown in Tables 7.2–7.5.

Polyamidoamine (PAMAM)

Since dendrimers are being investigated for potential drug delivery roles, cytotoxicity studies must investigate both the properties of the parent molecule and that of the drug- or gene-conjugated molecule. In this subsection several cationic PAMAM dendrimers conjugated with various therapeutics are surveyed.

Cationic PAMAM: Effect of Generation and Dosage

Haensler and Szoka (1993) investigated the effects of cationic PAMAM generation 2–10 (G2–10) (Figure 7.4) in the monkey fibroblast cell line CV-1. The dendrimer's diameter, dose, and the presence/absence of DNA were factors determining the toxicity of cationic PAMAM toward the adherent CV-1. Cells were incubated with 0–60 μg of poly-L-lysine (PLL) or PAMAM G6 for 5 h in serum-free media followed by culture in serum-containing media for 48 h without dendrimer. The effect upon CV-1 was quantified by measuring total cellular protein in addition to the MTT dye reduction assay, which measures mitochondrial activity through reduction of MTT into formazan. PAMAM G6 was significantly less toxic than the polycationic polymeric control PLL. The lethal dose for 50% of the cells (LD_{50}) was above 300 μg/ml for PAMAM G6 and was 25 μg/ml for PLL. When DNA was complexed with the PAMAM G6 dendrimer in a 10:1 ratio of primary amines:nucleotide, the LD_{50} of G6 increased nearly threefold to 100 μg/ml while that of PLL remained unchanged. Another

Table 7.2 Summary of in vitro studies on cationic polyamidoamine (PAMAM), polyethyleneimine-based diaminobutane (DAB) dendrimers.

Dendrimer	Generation Tested (G)	Species	Cells	Assay	Reference
	G2 - 10	monkey	fibroblast CV-1	Cytotoxicity	Haensler & Szoka, 1993
	G5	sheep	red blood cells	Hemolysis	Plank et al, 1996
	G3, 5 & 7	Chinese har	lung fibroblast V79	Cytotoxicity	Roberts et al., 1996
	G4	rat	Extensor digitorum longus myocytes	Cytotoxicity	Brazeau et al., 1997
	G2 - 4	murine	B16F10 melanoma	Cytotoxicity	Malik et al., 2000
	G5	human	HeLa cervical cancer	Cytotoxicity	Yoo & Juliano, 2000
	G5 Superfect	monkey	Cos-7 kidney fibroblasts	Cytotoxicity	Gebhart et al., 2001
PAMAM	G0 - 4	human	Caco-2 intestinal adenocarcinoma	Cytotoxicity	El Sayed et al., 2002
	G3	murine rat	L929 fibroblasts red blood cells	Cytotoxicity Hemolysis	Fischer et al., 2003
	G2 -4	human	Caco-2 intestinal adenocarcinoma	Cytotoxicity	Jevprasesphant et al., 2003
	G5-PEG triblock	human	293 kidney RAW 264.7 macrophage-like	Cytotoxicity	Kim et al., 2004
	G5	murine	NIH/3T3 fibroblasts BNL CL.2 hepatocytes	Cytotoxicity	Kuo et al., 2005
DAB	G2-4	murine	B16F10 melanoma	Cytotoxicity	Malik et al., 2000
	G1 - 5	human	A431 epidermoid cancer	Cytotoxicity	Zinselmeyer et al., 2002
	G5	murine	RAW 264.7 macrophage-like	Cytotoxicity	Kuo et al., 2005
	Q1 - 4	human	A431 epidermoid cancer	Cytotoxicity	Schatzlein et al., 2005
DAE	G1-3	murine	B16F10 melanoma	Cytotoxicity	Malik et al., 2000

Table 7.3 Summary of *in vitro* studies on anionic Polyamidoamine (PAMAM) & Polyethyleneimine-based diaminobutane (DAB) dendrimers.

Dendrimer	Generation Tested (G)	Species	Cells	Assay	Reference
PAMAM	G1.5 - 7.5	murine	B16F10 melanoma	Cytotoxicity Hemolysis	Malik et al., 2000
DAB	G1.5 - 3.5	murine	B16F10 melanoma	Cytotoxicity Hemolysis	

study investigated the effect of G3, G5, and G7 on V79 Chinese hamster lung fibroblasts at 4 and 24 h (Roberts, Bhalgat, & Zera, 1996). Three concentrations of dendrimer were used: 100 nM, 10 μM, or 1 mM. After treatment the adherent cells were harvested from the surface, counted, and re-plated for 6–7 days at which time the cells were stained with crystal

Table 7.4 Summary of *in vivo* studies on cationic Polyamidoamine (PAMAM) & Polyethyleneimine-based diaminobutane (DAB) dendrimers.

Dendrimer	Generation Tested (G)	Animal models	Assay	Reference
PAMAM	G3, 5 & 7	Swiss-Webster mice	Biodistribution & toxicity	Roberts et al., 1996
	G3	rats	Accumulation	Margerum et al., 1997
	G3 & 4	Wistar rats	Biodistribution & toxicity	Malik et al., 2000
	G4	nude mice	Blood half-life	Kobayashi et al., 2001
DAB	G1 - 4	BALB/c mice	Toxicity	Schatzlein et al., 2005

Table 7.5 Summary of *in vivo* studies on anionic Polyamidoamine (PAMAM) dendrimers.

Generation Tested (G)	Animal models	Assay	Reference
G2.5, 3.5 & 5.5	Wistar rats	Blood clearance & accumulation	Malik et al., 2000
G3.5	C57 mice	Toxicity	Matsumura & Maeda, (1986)

violet dye and colonies of $\geq$50 cells were counted. Not surprisingly a concentration- and generation-dependent toxicity was observed. PAMAM G3 was highly toxic (<10% survival) only at the 1 mM dosage while G5 was toxic at 10 μM. G7 was toxic at all concentrations tested. Increased culture time of 24 h vs 4 h did not significantly increase toxicity to V79 cells. These results coincide with observations by Tomalia and co-workers (1990) that below G3 PAMAM is more flexible and possesses a 3-D conformation similar to a starfish. The addition of two generations of linear branching restricts the conformation of PAMAM G5 and above into a rigid sphere. Haensler and Szoka (1993) theorized that the spherical PAMAM may be more efficient at destabilizing a cell's plasma membrane while Roberts and co-workers (1996) proposed the generation-dependent increase in toxicity was due primarily to the increasing cationic nature of the dendrimer surface.

PAMAM G2–4 was investigated for toxicity against B16F10 murine melanoma cells (Malik, Wiwattanapatapee, Klopsch, Lorenz, Frey, Weener, Meijer, Paulus, & Duncan, 2000). Dendrimers were cultured with cells in serum-containing media for 67 h before the addition of MTT dye for the last 5 h for a total of 72 h. PAMAM G2–4 showed lower toxicity to B16F10 than PLL at concentrations below 0.1 mg/ml. PAMAM G1 showed no concentration-dependent toxicity toward B16F10. PAMAM G3 and G4 showed similar IC_{50} values as the PLL-positive control from 0.1 to 5 mg/ml. In addition, there was a weak generation-dependent toxicity observed for PAMAM. Morphological changes determined by scanning electron microscopy were not present for B16F10 treated with PAMAM at 1 h but were apparent by 5 h. The generation of PAMAM was not noted. Thus the generation and concentration effects observed by Malik et al. (2000) are in support of previous conclusions.

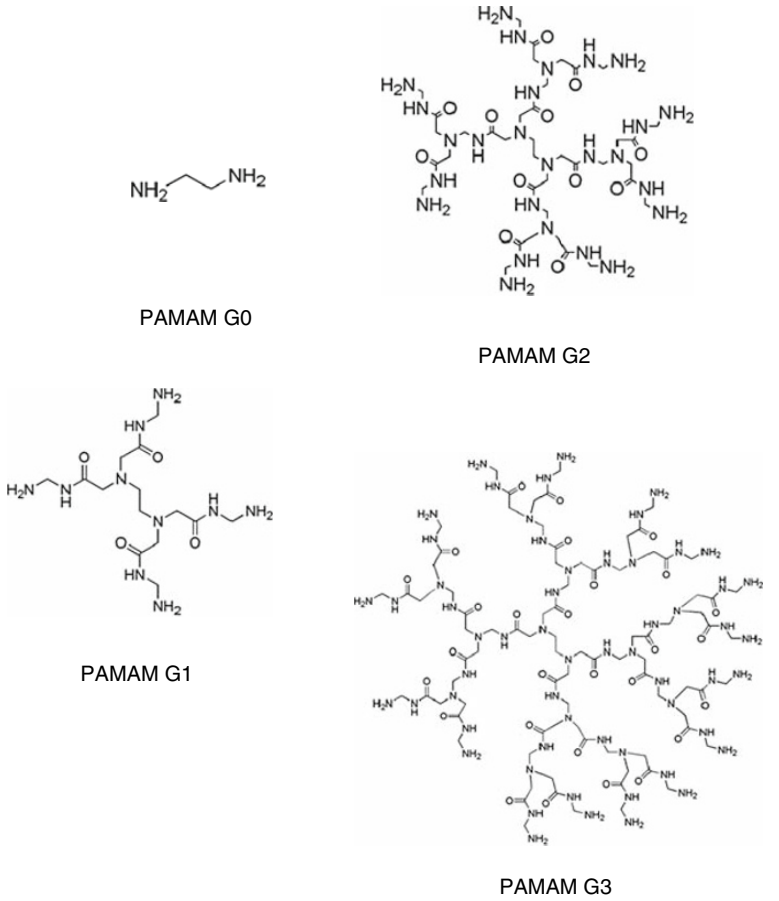

Figure 7.4 Cationic polyamidoamine (PAMAM) generation (G) 0–3 dendrimers.

MTT dye reduction was also used to assess the toxicity of PAMAM G3 dendrimers to L929 mouse fibroblastic cells (Fischer, Li, Ahlemeyer, Krieglstein, & Kissel, 2003). L929 were treated with PAMAM G3 for 3, 12, or 24 h at which time the cells were cultured with MTT for 4 h. PAMAM G3 showed no toxic effects at 0.01 or 0.1 mg/ml at 3, 12, or 24 h. PAMAM G3 showed >80% L929 viability at 3 and 12 h with a slight decrease at 24 h. PAMAM G3 showed significantly higher viability than PLL or linear polyethyleneimine (PEI) at 0.1 and 1 mg/ml and all time points. Both PLL and PEI at 0.1 and 1 mg/ml were highly toxic (Fischer et al., 2003). The extent of membrane damage caused by various polycationic polymers was also investigated at 0.01, 0.1, and 1 mg/ml via lactate dehydrogenase (LDH) release measured at 0, 30, and 60 min for each concentration. PAMAM G3 did not induce significant LDH levels whereas PLL significantly compromised the cellular membrane at 0.01 mg/ml after 30 min. PEI affected membrane integrity at 0.01 mg/ml after 60 min. Membrane destabilization was more pronounced at 0.1 and 1 mg/ml. It is important to note that the PLL and PEI tested here were the linear polymers and not dendrimer formulations. Thus the PAMAM G3

with tertiary amine groups on its surface showed less toxicity and membrane damage than PLL or PEI. However, this data is difficult to compare against other cytotoxicity studies because the pH and osmolarity of the cell culture medium was adjusted to pH 7.4 and 295 mosm/kg whereas none of the other studies mentioned any culture adjustments.

Caco-2 human intestinal adenocarcinoma cells were incubated with 0.1, 1, or 10 mM PAMAM G0–4 and LDH leakage assayed at 90, 150, and 210 min (El-Sayed, Ginski, Rhodes, & Ghandehari, 2002). LDH leakage of Caco-2 caused by PAMAM G0–4 was observed to increase with generation. G0 and G1 did not induce significant LDH leakage at any concentration tested up to 210 min. PAMAM G2 caused significant membrane damage only at 10 mM after 210 min. PAMAM G3 resulted in significant LDH levels at all concentrations only at 210 min while G4 caused extensive membrane destabilization at all concentrations and time points (El-Sayed et al., 2002). LDH measures damage to the plasma membrane, which allows the LDH to leak from the cell, in contrast to MTT, which measures metabolic activity in the mitochondria. Using parallel assays can confirm the true effect of a particular treatment or reveal potentially misleading interactions. As shown by El-Sayed et al. (2002) and Fischer et al. (2003), LDH confirmed the previous observations by MTT that PAMAM exhibits generation- and dose-dependent toxicity to cells in vitro.

While most research has focused solely on metabolic effects of the cationic dendrimers via MTT dye reduction, Kuo and co-workers (2005) investigated the mechanism of cell death in RAW 264.7 murine macrophage-like cells caused by PAMAM G5. Cytotoxicity was assayed by MTT dye assay and membrane damage measured by LDH release after exposure to the dendrimer for 24 h; 264.7 viability decreased significantly at 0.01 mg/ml with highly toxic effects at 0.1 and 0.2 mg/ml. A DNA fragmentation assay showed a DNA ladder consistent with DNA fragmentation during apoptosis in PAMAM G5-treated cells indicating the macrophages underwent programmed cell death rather than necrotic lysis (Kuo et al., 2005). Interestingly, NIH/3T3 and BNL CL.2 murine fibroblasts and liver cells, respectively, were not sensitive to cationic PAMAM dendrimer-induced apoptosis (Kuo et al., 2005). Previously murine macrophages were found to be significantly more sensitive to cationic polymer-induced toxicity than rat hepatocytes or bovine microvessel endothelial cells (Choksakulnimitr, Masuda, Tokuda, Takakura, & Hashida, 1995). Thus relative toxicity of the same polymer to different cell lines must be considered when comparing toxicity results and doses from different studies using various cells from different animal or human sources.

Initial toxicity screening allows researchers to predict the expected behavior of a given compound in vivo before proceeding with further testing. The interaction between cationic PAMAM dendrimers and blood cells is critical to their in vivo efficacy because dendrimers ultimately will circulate in the blood independent of the route of administration. Therefore the hemolytic properties of dendrimers are of particular interest. PAMAM G3 dendrimers at 0.01, 0.1, 5, and 10 mg/ml were incubated with red blood cells isolated from Wistar rats for 60 min (Fischer et al., 2003). The concentration of hemoglobin as detected by spectrophotometry was

less than 10% of the Triton X-100 positive control for all PAMAM concentrations tested and was therefore deemed non-toxic. While the data was obtained in triplicate no other time points or generations of PAMAM were tested. Malik and co-workers (2000) performed a more comprehensive study of the hemolytic properties of PAMAM G2–4, which showed both dose- and generation-dependent hemolysis after 1 h. Interestingly, PAMAM G1 showed no dose- or generation-dependent hemolysis, which may be due to its small molecular weight and low surface charge. This observation also eliminates the possibility of core-induced toxicity at low PAMAM generations. Scanning electron microscopy data obtained on these rat red blood cells showed significant morphological change at doses as low as 10 μg/ml for PAMAM contrasting the spectrophotometer data that showed hemolysis only at doses above 1 mg/ml. At 1 mg/ml red blood cells also showed more aggregation likely due to dendrimer cross-linking (Malik et al., 2000). Altered morphology can have significant impact upon red blood cell function in vivo as shown by the single amino acid mutation leading to sickle cell anemia. These hemolysis results highlight the importance of multiple assays to assess in vitro behavior. The spectrophotometer measurements did not indicate any cytotoxic effects; however, the scanning electron microscopy photos clearly showed a difference in morphology indicative of cell membrane damage and cell death (Malik et al., 2000).

Cationic PAMAM: Effect of Conjugated Molecules

The effect of PAMAM G4 with and without plasmid DNA (pDNA) upon extensor digitorum longus (EDL) muscles from Sprague–Dawley rats was calculated by total creatine kinase release determined at 30, 60, and 90 min by spectrophotometry (Brazeau, Attia, Poxon, & Hughes, 1998). At 1 mg/ml naked PAMAM G4 and G4-pDNA (3:1 w:w) showed similar toxicity to EDL muscle cells. However, naked G4 at 5 mg/ml was three times more myotoxic than G4-pDNA (3:1 w:w). A potential charge reducing complex might be formed upon addition of pDNA, or a change in particle size potentially leading to compaction similar to DNA on histones may lead to this decreased toxicity. pDNA is also a possible free radical scavenger thereby decreasing oxidative damage to the cells. Dendrimers stimulated the highest release of creatine kinase followed by PLL and liposomes. This decrease in toxicity of negatively charged pDNA complexed with the cationic PAMAM dendrimer supports Roberts et al. (1996) hypothesis that cytotoxicity is surface charge dependent.

Yoo and Juliano (2000) used PAMAM G5 conjugated to Oregon green 488 (G5-Org) fluorophore to study the cellular localization of dendrimers compared to their cargo. HeLa cells were incubated for 24 h with 30% fetal calf serum and without serum in the presence of G5-Org at which time the viability of the cells was determined via MTT dye reduction. Viability increased significantly for both the naked and oligonucleotide-conjugated G5-Org cultured with serum vs without. Interestingly, 30% serum decreased oligonucleotide delivery to the cells as determined by luciferase activity compared to the absence of serum but was similar to commercially available PAMAM dendrimer known as Superfect^{TM}. The hydrophobic Oregon green 488 fluorophore sufficiently shields the cationic charge on

the surface of Superfect™ to decrease its toxicity (Yoo & Juliano, 2000). The cytotoxicity of Superfect™ toward Cos-7 monkey kidney fibroblasts was investigated at different cell confluency and time points (Gebhart & Kabanov, 2001). Cos-7 at 40, 70, or 90% confluency were exposed to Superfect™ for 2 or 4 h after which the cells were grown in serum-containing media for 72 h before MTT analysis. Approximately 80% viability was observed for 40, 70, or 90% confluency Cos-7 at 2 and 4 h. This relatively low toxicity is beneficial because transfection increased significantly between 2 and 4 h. No other dendrimers or PAMAM generations were tested limiting the ability of these findings to support the generation- and concentration-dependent toxicity previously observed.

Cationic PAMAM: Effect of PEGylation or Other Surface Modification

The Caco-2 cell line was also used to investigate the toxicity of PEG or lauroyl fatty acid chain surface-modified PAMAM G2–4 dendrimers (Jevprasesphant, Penny, Jalal, Attwood, McKeown, & D'Emanuele, 2003). Consistent with previous findings, unmodified PAMAM dendrimers showed both a generation- and concentration-dependent cytotoxicity toward Caco-2. Viability was measured by MTT after 3 h of exposure to 90% confluent cells and 4 h of culture with both dendrimer and MTT. Surface modification of the tertiary amine groups on PAMAM G3 and G4 with six lauroyl chains reduced toxicity an order of magnitude compared to unmodified PAMAM G3 or G4. While six lauroyl chains showed marked reduction in PAMAM G3 and G4 toxicity, the addition of nine lauroyl chains to G2–4 resulted in similar toxicity as unmodified PAMAM G2–4. This difference in toxicity between six and nine lauroyl groups on the dendrimer surface is likely due to increased hydrophobic interaction with and destabilization of the plasma membrane. The addition of two PEG 2000 chains to PAMAM G4 had no effect on toxicity; however, four PEG 2000 chains resulted in a near sixfold reduction in toxicity. This PEG-dependent reduction in toxicity is consistent with previous findings that shielding the surface charge decreases toxicity. The two PEG chains likely did not sufficiently shield the charge amine groups on the PAMAM dendrimer. The reduction in toxicity shown by Jevprasesphant et al. (2003) reveals that shielding charge on the dendrimer surface via surface modification plays a significant role in toxicity but molecular weight and architecture are still important factors.

A PAMAM–PEG–PAMAM triblock copolymer dendrimer was synthesized to further investigate the impact of PEG modification on biocompatibility (Kim, Seo, Choi, Jang, Baek, Kim, & Park, 2004). Transformed human kidney 293 cells were exposed to PAMAM–PEG–PAMAM G5 dendrimer for 4 h at 70–80% confluency followed by 2 h incubation with MTT and cell lysis overnight in detergent. The copolymer G5 dendrimer showed no toxicity up to 0.15 mg/ml whereas PAMAM G4 showed slight toxicity (~80% viability) up to 0.15 mg/ml. Linear PEI (25 kDa) showed significant toxicity to 293 cells at 0.05 mg/ml. The PAMAM–PEG–PAMAM triblock dendrimer study did not investigate higher generation or higher concentrations to determine the role inserting PEG into the dendrimer architecture has upon biocompatibility compared to unmodified PEG. Thus the conclusions drawn by Kim et al. (2004) are

limited in their applicability to understanding the effect of molecular weight, surface functionality, and surface charge.

Cationic PAMAM: Immune Response and* In Vivo *Reaction

In addition to non-toxic and non-hemolytic, a dendrimer for drug delivery applications must not elicit an excessive immune response. A dendrimer with low toxicity and hemolysis but high immunogenicity could lead to death upon administration in the extreme case or rapid elimination in less severe cases. Thus immunogenicity is a critical determinant in the success of any drug delivery vehicle. Hemolysis of antibody-sensitized sheep red blood cells by complement proteins in serum was used to measure the complement activation induced by PAMAM G5 with and without complexation to DNA (Plank, Mechtler, Szoka, & Wagner, 1996). The complement system is part of the innate immune system capable of triggering non-specific cell lysis via formation of a membrane attack complex that forms a pore in plasma membranes. Complement proteins adsorb onto the surface of the dendrimer and are depleted from the serum. The lower concentration of complement proteins then induces less hemolysis in a dose-dependent manner allowing researchers to gauge the extent of complement activation. The hemoglobin released from red blood cell lysis via the membrane attack complex can be measured using a spectrophotometer to determine the extent of complement activation. No complement activation was detectable at a charge ratio of 1:1; however, complement activation increased with the charge ratio reaching a maximum with only PAMAM G5 present (Plank et al., 1996). The charge ratio of DNA to dendrimer thus determines complement activation supporting the previous data that charge is important in determining the host response.

In vitro assays such as cytotoxicity and hemolysis provide information to guide researchers toward the best application for a particular dendrimer formulation. The cytotoxicity data guides dosage selection while hemolysis data influences surface modification and dosage frequency among other factors. The in vivo biodistribution of dendrimers is critical to therapeutic efficacy, toxicity, and morbidity. If a particular dendrimer formulation stimulates red blood cell aggregation an embolism, or clot, can form leading to entrapment in the lungs or brain. Also, many polymer therapies fail in vivo testing because of excessive accumulation and toxicity in vital organs such as the kidneys and liver. Thus animal testing is required to obtain preliminary data about biodistribution, accumulation, and toxicity before pursuing further experiments focusing on therapeutic efficiency. The in vivo toxicity of intraperitoneal (ip) ^{14}C-labeled PAMAM G3, 5, or 7 dendrimers at 5×10^{-6}, 5×10^{-5}, or 5×10^{-4} mmol/kg after 7 or 30 days and 5×10^{-4} mmol/kg at 6 months was investigated in Swiss–Webster male mice (20 g) (Roberts et al., 1996). No change in body weight or behavior was observed; however, one mouse in the 7-day group died 24 h after injection with G7 at the highest dose of 45 mg/kg (5×10^{-4} mmol/kg). No further investigation into the specific cause of death was performed. Mice in the 6-month group were investigated for the long-term effects of weekly 5×10^{-4} mmol/kg ip injections of G3, G5, and G7; however, the G7 dendrimer dosage was lowered to 5×10^{-5} mmol/kg after one mouse died 24 h after the initial dose. As with the 7- and 30-day groups, there was no change

in weight compared to the control group after 6 months. Interestingly, all of the liver samples obtained from the 6-month group exhibited liver vacuolization but no further investigation was performed (Roberts et al., 1996). This vacuolization is indicative of lysosomal storage instead of degradation (Duncan & Izzo, 2005). In addition to the overall toxicity the biodistribution of these PAMAM dendrimers was investigated using ^{14}C-labeled PAMAM G3, 5, or 7 dendrimers at 0.05–0.25 μCi ^{14}C ($2–6\times10^{-4}$ mmol/kg). PAMAM G3 and G5 showed similar liver accumulation up to 48 h and were higher than G7, which remained relatively constant. No difference in kidney or spleen accumulation was found. G5 exhibited slightly higher pancreatic levels than G3 or G7 but were not significant. Interestingly, the G7 dendrimer was primarily excreted in urine at 2, 4, and 8 h. After 8 h urine excretion of G7 mimicked that of G3 and G5, which remained constant over 48 h. Significant differences in the amount of G3 pancreatic accumulation was observed between two independent trials. Roberts concluded that G3 and G5 appear to be suitable candidates for further in vivo therapies while G7 is not due to toxicity at high doses. This research supports previous findings that liposomes accumulate preferentially in the pancreas after ip but not iv injection (Goto & Ibuki, 1994). However, the number of surface-conjugated methyl groups required to gain a ^{14}C signal may influence the physicochemical properties of the dendrimer altering its biodistribution (Roberts et al., 1996). Therefore the distribution of ^{125}I core-labeled G3 and G4 PAMAM was observed at 1 h after ip or iv injection into male Wistar rats (250 g) (Malik et al., 2000). Blood levels were similar for both G3 and G4 after ip or iv injection. Ip injection resulted in similar liver accumulation for G3 and G4; PAMAM G4 showed significantly lower liver levels (~60% recovered dose) than G3 (~85%) after iv injection. The accumulation in other organs was not reported. It appears that surface charge and molecular weight have no role in liver accumulation after ip injection but do play a role after iv injection.

Conjugating PEG to PAMAM G3-gadolinium (Gd)-chelated dendrimers increased blood circulation significantly and decreased liver accumulation nearly fivefold at 7 days in rats (breed and weight were not reported) (Margerum, Campion, Koo, Shargill, Lai, Marumoto, & Sontum, 1997). The effects of PEG conjugation to ^{153}Gd-labeled PAMAM G4 were investigated as a potential means to increase blood half-life of the magnetic resonance imaging contrast agent 2-(*p*-isothiocyanatobenzl)-6-methyldiethylenetriaminepentaacetic acid (1B4M) conjugated to the dendrimer (Kobayashi, Kawamoto, Saga, Sato, Hiraga, Ishimori, Konishi, Togashi, & Brechbiel, 2001). Nude mice were injected with 1 μCi/200 μl for biodistribution studies and 3 μCi/200 μl for blood clearance. Conjugation of one or two 20,000 molecular weight PEG chains significantly increased blood circulation time compared to the non-PEGylated G4 dendrimer. Two PEG chains resulted in recovery of 20% of the initial dose/g in blood compared to 9% for one PEG chain and 2% for the non-PEGylated dendrimer. In addition, two PEG chains decreased liver accumulation compared to one PEG or non-PEGylated dendrimer, which showed similar levels. Two PEG chains did increase the accumulation in the lungs, which is likely due to increased molecular weight (96 kDa for two PEG chains vs 77 kDa for one PEG chain and 57 kDa for non-PEGylated

G4 PAMAM). PEGylating the G4-1B4M dendrimer also significantly increased blood clearance (Kobayashi et al., 2001). ^{153}Gd was continually excreted in the urine and feces of the mice with the PEGylated G4-1B4M showing higher excretion than the G4-1B4M parent molecule. Since the intent was to study blood retention of a contrasting agent no toxicity was obtained and only blood clearance investigated beyond 48 h. Nonetheless this data on PEG-modified PAMAM G4 is valuable for illustrating the in vivo effect of surface modification on blood clearance.

Anionic PAMAM: Effect of Generation, Dosage, and* In Vivo *Response

Much attention has focused on cationic PAMAM; however, anionic dendrimers can be synthesized that will not directly interact with the negatively charged plasma membrane (Figure 7.5). Malik et al. (2000) found that cationic PAMAM dendrimers showed toxicity to murine B16F10 melanoma cells above 100 μg/ml, but anionic PAMAM dendrimers G1.5–7.5 showed similar toxicity as the negative control dextran-treated cells up to 1 mg/ml. Anionic PAMAM dendrimers were not tested above 1 mg/ml. Similar results were found for anionic PAMAM G2.5 and G3.5 dendrimers in Caco-2 (Jevprasesphant et al., 2003). The cationic PAMAM G2–4 showed a concentration- and generation-dependent toxicity toward Caco-2 cells; however, G2.5 and G3.5 anionic PAMAM did not show significant toxicity even at

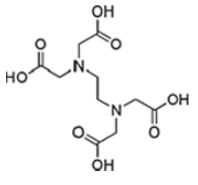

PAMAM G0.5

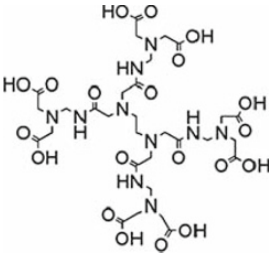

PAMAM G1.5

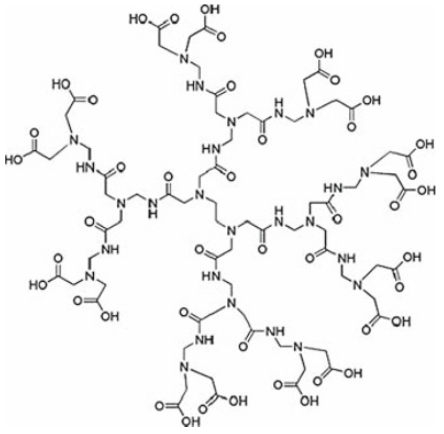

PAMAM G2.5

Figure 7.5 Anionic polyamidoamine (PAMAM) generation (G) 0.5–2.5 dendrimers.

1 mM. These findings are consistent with previous conclusions that surface charge plays an important role in the cytotoxicity of dendrimers. The cationic PAMAM can interact with a cell's negatively charged plasma membrane via electrostatic attraction and cause destabilization. The anionic PAMAM dendrimers are repulsed by the negatively charged plasma membrane preventing charge-dependent destabilization.

The negative surface charge on anionic PAMAM dendrimers showed similar results as the in vitro toxicity for decreasing hemolysis. Anionic PAMAM G1.5–3.5 showed no generation- or dose-dependent hemolysis up to 2 mg/ml after 1 h. However, PAMAM G7.5 and G9.5 were hemolytic at doses 2 mg/ml and above, which confirms the previously observed generational cytotoxicity likely due to the increase in molecular weight (212 and 852 kDa for G7.5 and G9.5, respectively vs <13 kDa for G1.5–3.5) and size. Anionic PAMAM G3.5 incubated with rat red blood cells for 24 h did not cause any dose-dependent increase in hemolysis (Malik et al., 2000). PAMAM G3.5–9.5 showed no morphological changes up to 2 mg/ml via scanning electron microscopy supporting the spectrophotometer measurements. Thus even at high concentrations anionic PAMAM showed little hemolytic properties. This lack of hemolysis further supports the theory that positively charged molecules destabilize the membrane leading to cell lysis since cationic and anionic PAMAM dendrimers share similar architecture but differing functional groups.

Based on the low in vitro toxicity and hemolytic properties of anionic PAMAM dendrimers, one would expect little to no in vivo toxicity even at high doses. Anionic PAMAM G2.5, 3.5, or 5.5 radiolabeled with ^{125}I were injected either ip or iv into Wistar rats (250 g) with blood clearance and liver accumulation assayed at 1 h (Malik et al., 2000). IV injection exhibited consistent blood levels recovered for G2.5, 3.5, and 5.5. G2.5 showed slightly higher blood levels than G3.5 or G5.5 at 1 h after ip administration. All three PAMAM dendrimers showed higher blood levels after ip injection than iv. Correspondingly liver levels for iv-administered PAMAM G2.5, 3.5, or 5.5 were higher than those for the respective ip-injected dendrimer indicating the liver may play a role in anionic PAMAM clearance. PAMAM G3.5 showed lower hepatic accumulation upon conjugation to platinum compared to the unconjugated PAMAM G3.5 dendrimer (Malik et al., 2000). Thus both positive and negative surface charge appears to play some role in localizing PAMAM dendrimers to the liver as evidenced by G3.5-platinate and cationic PAMAM findings and the PAMAM G3 and G4 results (Malik et al., 2000). The overall tolerability of PAMAM G3.5 was further illustrated by Matsumura and Maeda (1986). C57 mice with B16F10 tumors dosed with 95 mg/kg of PAMAM G3.5 via ip injection showed no weight change. This relatively high dose shows the comparatively low toxicity of anionic dendrimers compared to cationic, which showed lethality at 45 mg/kg with PAMAM G7. This difference appears to be driven largely by surface charge over molecular weight, size, and architecture.

PEI Dendrimers

In addition to PAMAM, PEI-based dendrimers have been investigated. These dendrimers differ in their core and dendrons from PAMAM.

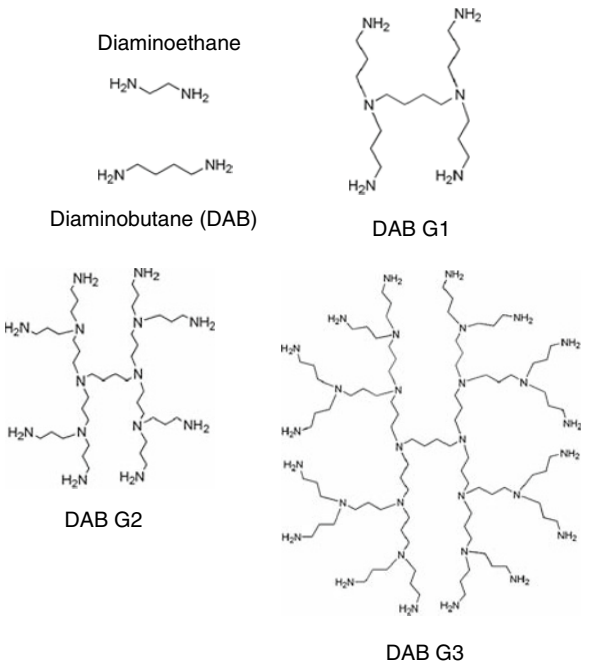

Figure 7.6 Cationic polyethyleneimine-based diaminobutane (DAB) generation (G) 0–3 dendrimers.

Diaminobutane (DAB) and diaminoethane (DAE) are the two most commonly used PEI-based dendrimer cores (Figure 7.6).

Cationic PEI: Effect of Generation, Dosage, and* In Vivo *Response

Malik and colleagues (2000) observed that DAB G2–4 or DAE core G1–3 showed lower toxicity to B16F10 than PLL at concentrations below 0.1 mg/ml. DAB G2–4 and DAE G3 showed similar inhibitory concentrations for half the cells (IC_{50}) as the PLL-positive control from 0.1 to 5 mg/ml. In addition, there was a weak generation-dependent toxicity observed for DAB and DAE dendrimers toward B16F10. Electron microscopy showed morphological changes in B16F10 after 1 h at concentrations as low as 0.001 mg/ml for DAB and DAE. However, significant morphological changes were seen at 1 mg/ml indicating toxicity for DAB and DAE. The generation of the dendrimers observed was not noted. PAMAM dendrimers did not show any morphological changes after 1 h demonstrating that architecture contributes to in vitro toxicity as PAMAM, DAB, and DAE have similar surface charge and functional groups but DAB and DAE are approximately half the molecular weight for a given generation.

In addition to PAMAM G5, Kuo et al. (2005) investigated the effect of PEI-based DAB G5 upon RAW 264.7. Viability decreased significantly at 0.01 mg/ml with highly toxic effects at 0.1 and 0.2 mg/ml. The results were nearly identical for PAMAM and DAB G5. LDH release corresponded to the increased toxicity with a significant LDH release increase at 0.1 mg/ml for both PAMAM G5 and DAB G5. A DNA fragmentation assay showed a DNA ladder consistent with DNA fragmentation during apoptosis in RAW 264.7 treated with DAB G5. These cells also exhibited a higher sub-G1 population than PAMAM G5 evidenced by higher propidium iodide

staining further supporting the apoptosis conclusion. While B16F10 appear sensitive to changes in architecture, 264.7 macrophages are more sensitive to surface charge, which may stem from their phagocytic role in the reticuloendothelial system (Kuo et al., 2005). In contrast to the dose- and generation-dependent hemolysis after 1 h caused by exposure to PAMAM G2–4, PEI-based dendrimers DAB G2–4 and DAE G1–3 exhibited only dose-dependent hemolysis up to 6 mg/ml at 1 h. This difference in hemolysis was attributed to a difference in molecular weight for a given number of surface groups (i.e., charge) and the presence of different interior functional groups such as secondary or tertiary amines (Kuo et al., 2005).

PEI-based DAB dendrimers showed increasing toxicity to A431 human epidermoid cancer cells with increasing generation from G1 to G5 with the exception of G1, which was more toxic than G2 but less toxic than G3 (G2 < G1 < G3 < G4 < G5) (Zinselmeyer, Mackay, Schatzlein, & Uchegbu, 2002). Therefore the previous observation by Roberts and co-workers (1996) that increasing generation show increasing toxicity is further supported and appears to be based primarily on surface charge and molecular weight. Complexing DAB G1 and G2 with DNA (5:1 DAB:DNA w:w) significantly reduced toxicity to A431 fourfold and twofold, respectively. There was little change in toxicity at higher generations (G3 and G4) complexed with DNA. Therefore with a 5:1 w:w ratio of DAB:DNA toxicity toward A431 is generation dependent. As a result of this lowered toxicity at lower generations, DAB G1–3 showed higher DNA transfection rates than G4 and G5 (Zinselmeyer et al., 2002). The reduction of toxicity resulting from complexing cationic dendrimer to anionic DNA also supports the theory that cationic dendrimers exhibit cytotoxicity through interaction with cellular anions critical for viability. This data was obtained by MTT after A431 were exposed to DAB and DAB–DNA for 4 h followed by fresh media for 72 h. MTT was incubated with the cells for 4 h before obtaining absorbance data.

The effect of tertiary amine groups on DAB G1–4 was compared against quaternized DAB dendrimers (Q1–4) at coinciding generations to better characterize the role surface charge plays in toxicity (Schatzlein, Zinselmeyer, Elouzi, Dufes, Chim, Roberts, Davies, Munro, Gray, & Uchegbu, 2005). DAB Q1 and Q2 increased cytotoxicity compared to G1 and G2; Q3 showed no change from G3 while Q4 showed a slight decrease in IC_{50} value compared to DAB G4. The effect on A431 cytotoxicity of complexing Q1–4 with DNA was also compared against G1–4. The IC_{50} value for Q1:DNA 5:1 w:w was higher than that for DAB G1:DNA 5:1 meaning the quaternized DAB was less toxic. DNA in a 5:1 w:w ratio decreased the IC_{50} value for Q2 to that of G2 without DNA but was still approximately half the value of G2:DNA 5:1. Toxicity data for Q3:DNA was only obtained at 3:1 ratio but was threefold lower than Q3 without DNA and G3. Thus the IC_{50} value for Q3:DNA may partially be the result of lower dendrimer concentration in the sample. The IC_{50} value for Q4:DNA 5:1 was 33 μg/ml compared to 11 μg/ml for Q4 and 5.7 μg/ml for DAB with or without DNA. These findings support the observation that shielding the surface of cationic dendrimers by complexation with anionic compounds such as DNA decreases their toxicity.

The effect of surface charge for cationic polymers was further investigated in vivo by testing the effect of quaternizing the terminal amine groups on the PEI-based dendrimer DAB G1–4 (Schatzlein et al., 2005); 100 μg DAB G2:DNA at a 5:1 dendrimer nitrogen:DNA phosphate (N:P) injected intravenously was lethal to female BALB/c mice resulting in what the authors described as "embolism-like (rapid) death" (Schatzlein et al., 2005). Interestingly, the quaternized Q2 dendrimer:DNA conjugate at the same dose was not lethal. This decreased lethality was attributed to the quaternized dendrimer's increased ability to complex with DNA. This fact was reinforced by IC_{50} values that showed a sevenfold decrease in toxicity when the Q2 dendrimer was complexed with DNA (49 μg/ml without DNA vs 350 μg/ml with DNA). The Q2 dendrimer with 16 external quaternary amine groups was ideal because 14 moles of DNA phosphate were associated with each mole of dendrimer. Increasing the dendrimer size to Q3 with 32 external quaternary amines only resulted in 15 moles of DNA phosphate associated per mole dendrimer. Thus Q2 with 16 surface quaternary amine groups maximized DNA conjugation and hence charge shielding while minimizing molecular weight and size. The amine groups on DAB were quaternized by methylation resulting in a dendrimer structure similar to that used by Roberts et al. (1996) potentially explaining why Q16:DNA accumulated to a significant extent in the liver (Schatzlein et al., 2005). As was shown with the in vitro cytotoxicity data, shielding of external surface charge on dendrimers through complexation with DNA or via surface modification such as PEG grafting decreases in vivo toxicity and in the case of quaternized DAB G2 also increases gene transfer (Schatzlein et al., 2005).

Anionic PEI: Effect of Generation and Dosage

Changing surface charge from cationic to anionic decreased in vitro toxicity in PAMAM dendrimers. Therefore a similar decrease would be expected from PEI-based dendrimers based on previous observations that charge plays a large role in toxicity. DAB G1.5–3.5 also showed similar toxicity as dextran up to 1 mg/ml but were toxic to B16F10 at high doses near 10 mg/ml (Malik et al., 2000). This finding was confirmed by scanning electron microscopy, which showed no significant morphological changes in B16F10 cells except at the highest dose of DAB. Even at doses above 1 mg/ml, DAB and DAE anionic dendrimers were less toxic than PLL or the corresponding generation cationic PEI dendrimer. Thus a dynamic relationship between surface charge, size, and concentration are critical factors determining dendrimer toxicity. Surprisingly little hemolytic data is published for anionic PEI dendrimers. Anionic DAB G1.5–3.5 showed no generation- or dose-dependent hemolysis up to 2 mg/ml after 1 h in contrast to cationic DAB G2–4 and DAE G1–3 that showed dose-dependent toxicity. Cationic PAMAM G2–4 exhibited both generation- and dose-dependent toxicity. Therefore surface charge eliminates the dose-dependent hemolytic property while architecture suppresses the generation-dependent effect. There is a small variation in molecular weight between PEI and PAMAM dendrimers. Cationic PEI dendrimers are approximately half the molecular weight of the corresponding generation PAMAM dendrimer; anionic PEI is approximately 30% smaller than PAMAM at the same generation and surface charge (Malik et al., 2000).

Despite significantly lower toxicity more research has been performed with cationic than anionic dendrimers. The ease of cargo loading such as DNA is a major factor in this focus on cationic dendrimers. Electrostatic attraction complexes negatively charged DNA with positively charged dendrimer. Anionic dendrimers are more difficult to conjugate to DNA. Since gene delivery is a major research focus for dendrimers the focus is obviously on cationic dendrimers. Even more surprising is that there currently are no published in vivo studies using anionic DAB or DAE dendrimers despite their low toxicity. With the current emphasis on developing more elegant drug delivery systems this lack of data using anionic PEI dendrimers will not likely last.

Other Dendrimer Core Structures

Carbosilane-Based Dendrimers

Most dendrimer research has focused on PAMAM based on an ethylene diamine core or PEI built around either a diaminobutane or diaminoethane core. However, dendrimers are not limited to just these core structures. Carbosilane can be grafted with poly(ethylene oxide) (CSi-PEO) to form a dendrimer with PEO arms (Figure 7.7). These CSi-PEO G1 dendrimers showed significantly higher toxicity at doses above 1 mg/ml than the G2 dendrimer to B16F10 but were less toxic than PLL at all doses (Malik et al., 2000). This decreased toxicity for CSi-PEO G2 can be explained by the greater degree of shielding from the toxic core. However, these CSi-PEO dendrimers were not toxic to CCRF and human HepG2 hepatoma cells at doses up to 2 mg/ml. These findings again highlight the observation by Choksakulnimitr et al. (1995) that different cell lines demonstrate different levels of sensitivity to insult with polymers.

Further research into these carbosilane dendrimers investigated the effect surface charge has upon toxicity to primary cells obtained from human donors (Ortega, Bermejo, Chonco, de Jesus, de la Mata, Fernandez, Flores, Gomez, Serramia, & Munoz-Fernandez, 2006). Carbosilane G2 dendrimers with surface amine groups (8 or 16) quaternized with methyl iodide showed similar toxicity to peripheral blood monoculear cells at 1, 5, 10, 20, or 100 μM after 48 h incubation. Mitochondrial activity and thus viability were determined by MTT dye reduction after 4 h incubation with the MTT dye. Carbosilane G2 dendrimer with 8 or 16 surface methyl groups decreased mitochondrial activity from 80% at 1 μM to 30% at 5 μM. A dose of 10 μM showed a reduction to ~10% activity while 20 and 100 μM showed similar activities ~5% of the control cells without dendrimer exposure. These observations coincided with phase contrast microscopy of the peripheral blood monoculear cells. No morphological difference was observable between cells treated with 1 or 5 μM carbosilane G2 and the untreated control cells. However, above 10 μM membrane birefringence was significantly reduced and cell debris from dead peripheral blood monoculear cells was observable (Ortega et al., 2006). Peripheral blood monoculear cells are more difficult to culture and are more sensitive to dendrimers than immortalized cell lines, but the data obtained from these experiments is more physiologically relevant to in vivo behavior. As with the findings of Roberts et al. (1996) the addition of the

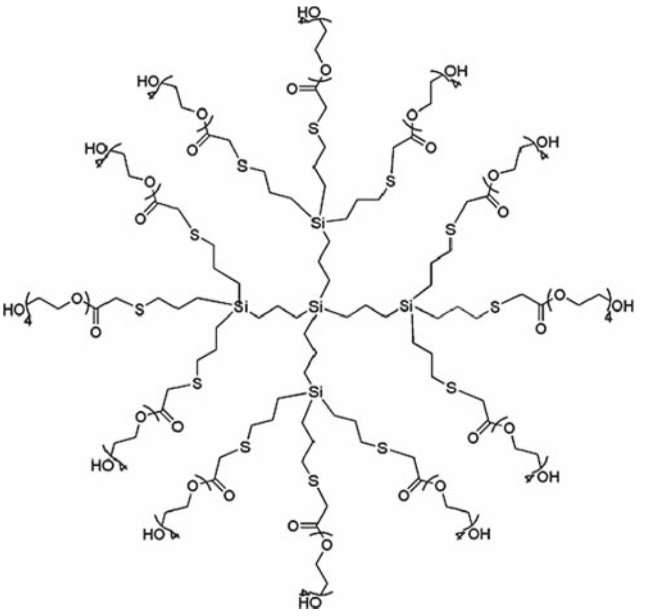

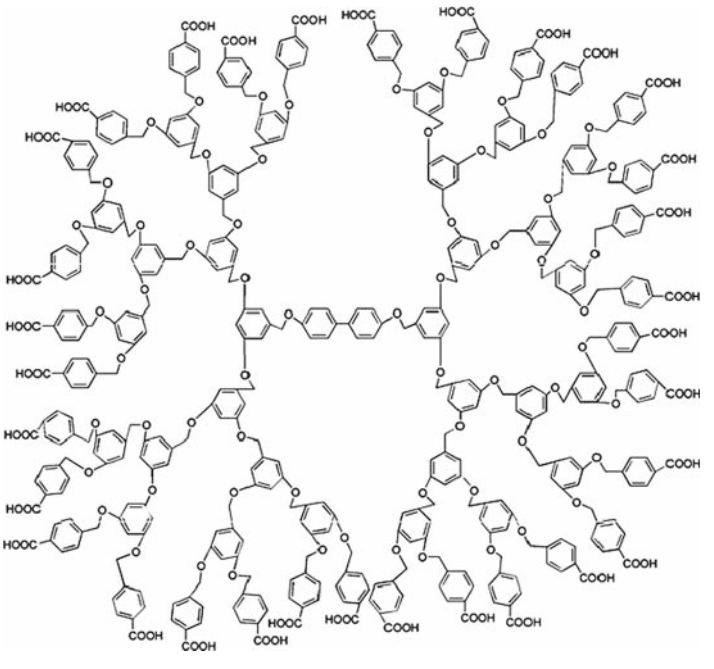

Figure 7.7 Carbosilane–polyethylene oxide and poly aryl ether dendrimers.

hydrophobic methyl group on the periphery of the dendrimer may affect the behavior of the quaternized carbosilane dendrimer. Despite promising in vitro toxicity data little in vitro hemolysis data is published for carbosilane dendrimers. These CSi dendrimers showed a similar hemolytic

behavior as the anionic dendrimers with $< 5\%$ hemolysis up to 2 mg/ml. More research into the effect of core toxicity, surface functional groups, and quaternization with hydrophobic methyl groups is needed prior to extensive in vivo testing.

Polyether-Based Dendrimers

De Jesus and co-workers (2002) conjugated methoxy-capped triethylene glycol to a propanoic acid-based polyester G4 dendrimer synthesized via the methodology of Inhre and co-workers (2002). The methoxy-capped triethylene glycol-modified polyester G4 dendrimer significantly increased toxicity of the dendrimers to B16F10 cells at doses higher than 5 mg/ml after 48 h. The toxicity of the modified dendrimer (11,500 Da) may be explained by the increase in molecular weight over the unmodified dendrimer (3790 Da). However, another dendrimer using three-armed PEO and G2 polyester dendrons (23,500 Da) showed similarity toxicity as the unmodified G4 polyester dendrimer (3790 Da) after 48 h at doses ranging up to 10 mg/ml. At 20 and 40 mg/ml this PEO-polyester G2 dendrimer showed significantly less toxicity toward B16F10 cells than the unmodified G4 polyester as determined by sulforhodamine B (SRB). De Jesus et al. (2002) theorized that PEO-polyester dendrimer appeared to inhibit growth of B16F10 resulting in the appearance of dendrimer-mediated toxicity as compared to the control. The ether and carbonyl nature of the backbone may also contribute to the cytotoxicity. Despite using the same cell line, the results found by De Jesus are difficult to compare to those by Malik because different cell viability assays were used (MTT vs sulforhodamine B assay), incubation time varied (48 h vs 72 h for Malik), and doses varied by nearly an order of magnitude. In addition, the doses used by De Jesus et al. (2002) are significantly higher than most experiments reviewed here with the exception of two in vivo tests discussed previously in this section.

A convergent poly aryl ether dendrimer was synthesized with either a carboxylate terminal group or malonate (Malik et al., 2000) (Figure 7.7). The poly aryl ether G2 dendrimers showed no dose- or concentration-dependent hemolysis after 1 h for either the carboxylate or malonate terminal groups, but both forms of G2 polyether dendrimer did cause complete hemolysis at $\geq$ 1 mg/ml after 24 h. The G0 dendrimer with carboxylate groups showed hemolysis at concentrations above 3 mg/ml at 1 h due to hydrophobic aromatic groups capable of interacting with the plasma membrane (Malik et al., 2000). As the generation increased to G2 these aromatic rings were buried more within the polyether dendrimer preventing interaction with cells making them less toxic. Thus even with anionic polyether dendrimers architecture plays an important role in toxicity and hemolysis (Malik et al., 2000).

Studies on the in vivo behavior of these higher generation anionic polyester and polyether dendrimers are limited. Polyester-based G4 dendrimers (MW 3790 Da) and three-armed PEG-G2 polyester dendrons (MW 23,500 Da) were iv injected into CD-1 nude mice at 1.3 g/kg (De Jesus et al., 2002). The unmodified polyester dendrimer showed immediate lethality in one mouse with no evidence indicating embolism. The second mouse was sacrificed at 24 h and showed no gross toxicity to its organs. The higher molecular weight dendrimer based on three-armed PEG was not lethal to either mouse, which may be due to its flexibility and low core toxicity. After

24 h neither mouse exhibited signs of gross toxicity to its organs. Based upon these results biodistribution studies were undertaken using ^{125}I-labeled dendrimer to determine localization. The polyester G4 dendrimer was excreted through the kidneys as expected for a small molecular weight compound and was completely eliminated by 4 h post-injection (De Jesus et al., 2002). The methoxy-capped triethylene glycol-modified version of the G4 polyester dendrimer was also renally excreted despite have a threefold higher molecular weight. After 30 min less than 5% of the methoxy-capped polyester dendrimer was detected in serum and was primarily excreted by 5 h post-injection. The three-armed PEG-based polyester dendrimer showed significant liver accumulation just 3 min post-injection. Liver levels remained high throughout the experiment with 53% of the injected dose still residing in the liver after 5 h. The three-armed PEG-based dendrimer could not be labeled using the same reaction mechanism as for G4 polyester dendrimer thus the ^{125}I was located on the surface of the dendrimer rather than on the core. Hydrolysis of the ^{125}I linkage was ruled out because liver accumulation was observed after just 3 min and radioactivity was detected in the high molecular weight fraction of G-50 spin columns (De Jesus et al., 2002). Further experiments were performed using this three-armed PEG-based polyester dendrimer conjugated to the potent chemotherapeutic drug doxorubicin. Polyester dendrimer–doxorubicin did not accumulate significantly in the lungs, heart, or liver in contrast to free doxorubicin, which is well known to accumulate in the heart and lungs. Thus this PEG-polyester-based dendrimer shows potential to increase therapeutic efficiency of doxorubicin without the toxicity and organ accumulation concomitant with administration of the free drug.

Melamine-Based Dendrimers

A triazine ring was used as the core for dendrimers based on melamine (Neerman, Zhang, Parrish, & Simanek, 2004). This core structure allows researchers to specifically tailor both the functional groups present on the dendrimer surface along with their spatial arrangement (Zhang, Jiang, Qin, Perez, Parrish, Safe, & Simanek, 2003). Neerman et al. used a G3 melamine dendrimer with amine functional groups and found that these dendrimers exhibited toxicity to Clone 9 rat liver cells at 0.1 mg/ml. This relatively high level of toxicity is likely due to a combination of the terminal amine groups and the architecture, which is rich in polyether bonds and triazole rings. The in vivo effects of these melamine dendrimers were also investigated (Neerman et al., 2004). Melamine G3 was found to be lethal at the extremely high dose of 160 mg/kg in male C3H mice at 6–12 h. Blood urea nitrogen was used to assess renal toxicity. No significant difference between the melamine G3 and the control group was found at 2.5, 10, or 40 mg/kg after 48 h or 6 weeks. The chronic time point taken at 6 weeks comprised three doses every 3 weeks for 6 weeks total. Alanine transaminase was used to assess liver function. Again no difference was found between G3 melamine treatment and the control at 2.5 and 10 mg/kg after 48 h or 6 weeks; however, there was a significant difference between both the 48 h and 6-week groups dosed at 40 mg/kg melamine G3 and PBS-treated mice. Thus melamine G3 is apparently not toxic to the kidney even at high doses and was confirmed through histological staining

with hemotoxylin and eosin (Neerman et al., 2004). However, liver toxicity is an issue at 40 mg/kg as evidenced by hepatocyte necrosis in histological slides. These findings are comparable to those by Roberts et al. (1996) who found that cationic PAMAM was relatively well tolerated even at high doses near 40 mg/kg except for G7.

Summary

Based on the studies presented, a complex combination of dendrimer architecture, molecular weight, and surface functionality/charge plays a role in toxicity in vitro. The effect on a specific cell model may be unique and cannot be extrapolated to other cell types. The behavior of dendrimers in vivo is less well defined and unified. In vitro and in vivo disconnect also exists. For example, cationic PAMAM dendrimers that show relatively high toxicity in vitro are reasonably tolerated in vivo even at high doses (Roberts et al., 1996; Malik et al., 2000; Neerman et al., 2004). Other groups have injected even higher doses of anionic dendrimer. PEG-G2 polyester dendrons (MW 23,500 Da) were iv injected into CD-1 nude mice at 1.3 g/kg with immediate lethality in one of two mice (De Jesus et al., 2002). In addition, the major focus of dendrimer research has focused on cationic PAMAM and PEI dendrimers with significantly fewer studies on anionic dendrimers or different architecture (Tables 7.2–7.5). The current body of work supports some generalized hypotheses. First, cationic surface charge increases toxicity through membrane destabilization. And second, the structure of the dendrons also plays a role in membrane destabilization as seen with the melamine dendrimer (Neerman et al., 2004) and polyether G0 dendrimer (Malik et al., 2000). However, more research is needed into the full mechanism underlying the complex interaction of dendrimer molecular weight, size, surface charge, and architecture.

Conclusions

More research has been performed on cationic dendrimer biocompatibility than bioMEMS or anionic dendrimer biocompatibility. A few general conclusions can be made regarding dendrimer structure, surface charge, and architecture, but more mechanistic research is needed to better understand the complex role these factors play. In addition, little standardized biocompatibility have been performed for bioMEMS and dendrimers. More conclusions regarding dendrimer biocompatibility could be drawn with more careful selection of cell model and culture conditions as evidenced previously and in Tables 7.2–7.5. Therefore more research adhering to the guidelines established by ISO 10993 and ASTM F748 will allow researchers to draw conclusions from similar experiments that are not currently available.

References

Allen, M., Butter, R., Chandra, L., Lettington, A., & Rushton, N. (1995). Toxicity of particulate silicon carbide for macrophage, fibroblasts and osteoblast-like cells *in vitro*. *Bio-medical Materials and Engineering,* 5, 151–9.

Amon, M., Bolz, A., & Schaldach, M. (1996). Improvement of stenting therapy with a silicon carbide coated tantalum stent. *Journal of Materials Science-Materials in Medicine,* 7, 273–8.

American Society for Testing Materials Standards International. (2004). ASTM F 748-04: Standard practice for selecting generic biological test methods for materials and devices. Retrieved October 20, 2006, from http://www.astm.org.

Bayliss, S.C. & Buckberry, L.D. (1999). A material for melding humans and machines. *Materials World,* 7, 213–5.

Bayliss, S.C., Heald, R., Fletcher, D.I., & Buckberry, L.D. (1999). The culture of mammalian cells on nanostructured silicon. *Advanced Materials,* 11, 318–21.

Bayliss, S.C., Buckberry, L.D., Harris, P.J., & Tobin, M. (2000). Nature of the silicon-animal cell interface. *Journal of Porous Materials,* 7, 191–5.

Bayliss, S.C., Harris, P.J., Buckberry, L., & Rousseau, C. (1997). Phosphate and cell growth on nanostructured semiconductors. *Journal of Materials Science Letters,* 16, 737–40.

Blattler, T., Huwiler, C., Ochsner, M., Stadler, B., Solak, H., Voros, J., & Grandin, H.M. (2006). Nanopatterns with biological functions. *Journal of Nanoscience and Nanotechnology,* 6, 2237–64.

Boas, U. & Heegaard, P.M.H. (2004). Dendrimers in drug research. *Chemical Society Reviews,* 33, 43–63.

Brazeau, G.A., Attia, S., Poxon, S., & Hughes, J.A. (1998). *In vitro* myotoxicity of selected cationic macromolecules used in non-viral gene delivery. *Pharmaceutical Research,* 15, 680–4.

Chen, H.Y., Elkasabi, Y., & Lahann, J. (2005). Surface modification of confined microgeometries via vapor-deposited polymer coatings. *Journal of the American Chemical Society,* 128, 374–80.

Chen, Z., Zhang, R.F., Kodama, M., & Nakaya, T. (1999). Preparations and properties of a novel grafted segmented polyurethane-bearing glucose groups. *Journal of Biomaterials Science-Polymer Edition,* 10, 901–16.

Chin, V.I., Taupin, P., Sanga, S., Scheel, J., Gage, F.H., & Bhatia, S.N. (2004). Microfabricated platform for studying stem cell fates. *Biotechnology and Bioengineering,* 88, 399–415.

Choksakulnimitr, S., Masuda, S., Tokuda, H., Takakura, Y., & Hashida, M. (1995). *In vitro* cytotoxicity of macromolecules in different cell culture systems. *Journal of Controlled Release,* 34, 233–41.

De Jesus, O.L.P, Ihre, H.R., Gagne, L., Frechet, J.M.J., & Szoka, F.C. (2002). Polyester dendritic systems for drug delivery applications: *in vitro* and *in vivo* evaluation. *Bioconjugate Chemistry,* 13, 453–61.

Duncan, R. & Izzo, L. (2005). Dendrimer biocompatibility and toxicity. *Advanced Drug Delivery Reviews,* 57, 2215–37.

Elam, J.H. & Nygren, H. (1992). Adsorption of coagulation proteins from whole blood on to polymer materials – relation to platelet activation. *Biomaterials,* 13, 3–8.

El-Sayed, M., Ginski, M., Rhodes, C., & Ghandehari, H. (2002). Transepithelial transport of poly(amidoamine) dendrimers across Caco-2 cell monolayers. *Journal of Controlled Release,* 81, 355–65.

Fischer, D., Li, Y., Ahlemeyer, B., Krieglstein, J., & Kissel, T. (2003). *In vitro* cytotoxicity testing of polycations: influence of polymer structure on cell viability and hemolysis. *Biomaterials,* 24, 1121–31.

Gebhart, C.L. & Kabanov, A.V. (2001). Evaluation of polyplexes as gene transfer agents. *Journal of Controlled Release,* 73, 401–16.

Gibbins, J.M. (2004). Platelet adhesion signaling and the regulation of thrombus formation. *Journal of Cell Science,* 117, 3415–25.

Goto, R. & Ibuki, Y.D. (1994). Tissue distribution of liposomes prepared from synthetic amphiphiles after intraperitoneal injection into mice. *Applied Radiation and Isotopes,* 45, 47–62.

Gourley, P.L. (2005). Brief overview of biomicronano technologies. *Biotechnology Progress,* 21, 2–10.

Haensler, J. & Szoka Jr., F.C. (1993). Polyamidoamine cascade polymers mediate efficient transfection of cells in culture. *Bioconjugate Chemistry,* 4, 372–9.

Hanein, Y., Pan, Y.V., Ratner, B.D., Denton, D.D., & Bohringer, K.F. (2001). Micromachining of non-fouling coatings for bio-MEMS applications. *Sensors and Actuators B-Chemical,* 81, 49–54.

Hiratsuka, Y., Miyata, M., Tada, T., & Uyeda, T.Q.P. (2006). A microrotary motor powered by bacteria. *Proceedings of the National Academy of Sciences of the United States of America,* 103, 13618–23.

Ihre, H.R., De Jesus, O.L.P., Szoka, F.C., & Frechet, J.M.J. (2002). Polyester dendritic systems for drug delivery applications: design, synthesis, and characterization. *Bioconjugate Chemistry,* 13, 443–52.

International Organization for Standards. (2003). Biological evaluation of medical devices. Retrieved October 20, 2006, from http://www.iso.org.

Ishikawa, M., Schmidtke, D.W., Raskin, P., & Quinn, C.A.P. (1998). Initial evaluation of a 290-μm diameter subcutaneous glucose sensor: glucose monitoring with a biocompatible, flexible-wire, enzyme-based amperometric microsensor in diabetic and nondiabetic humans. *Journal of Diabetes and Its Complications,* 12, 295–301.

Jevprasesphant, R., Penny, J., Jalal, R., Attwood, D., McKeown, N.B., D'Emanuele, A. (2003). The influence of surface modification on the cytotoxicity of PAMAM dendrimers. *International Journal of Pharmaceutics,* 252, 263–6.

Johansson, C.B., Hansson, H.A., & Albrektsson, T. (1990). Qualitative interfacial study between bone and tantalum, niobium or commercially pure titanium. *Biomaterials,* 11, 277–80.

Kaneda, Y. (2000). Virosomes: evolution of the liposome as a targeted drug delivery system. *Advanced Drug Delivery Reviews,* 43, 197–205.

Kim, K., Kim, C., & Byun, Y. (2001). Preparation of a dipalmitoylphosphatidylcholine/cholesterol Langmuir–Blodgett monolayer that suppresses protein adsorption. *Langmuir,* 17, 5066–70.

Kim, T.-I., Seo, H.J., Choi, J.S., Jang, H.-S., Baek, J.-U., Kim, K., & Park J.-S. (2004). PAMAM-PEG-PAMAM: novel triblock copolymer as a biocompatible and efficient gene delivery carrier. *Biomacromolecules,* 5, 2487–92.

Kobayashi, H., Kawamoto, S., Saga, T., Sato, N., Hiraga, A., Ishimori, T., Konishi, J., Togashi, K., & Brechbiel, M.W. (2001). Positive effects of polyethylene glycol conjugation to generation-4 polyamidoamine dendrimers as macromolecular MR contrast agents. *Magnetic Resonance in Medicine,* 46, 781–8.

Kotzar, G., Freas, M., Abel, P., Fleischman, A., Roy, S., Zorman, C., Moran, J.M., & Melzak, J. (2002). Evaluation of MEMS materials of construction for implantable medical devices. *Biomaterials,* 23, 2737–50.

Kros, A., Gerritsen, M., Sprakel, V.S.I., Sommerdijk, N.A.J.M., Jansen, J.A., & Nolte, R.J.M. (2001). Silica-based hybrid materials as biocompatible coatings for glucose sensors. *Sensors and Actuators B-Chemical,* 81, 68–75.

Kubo, K., Tsukasa, N., Uehara, M., Izumi, Y., Ogino, M., Kitano, M., & Sueda, T. (1997). Calcium and silicon from bioactive glass concerned with formation of nodules in periodontal ligament fibroblasts *in vitro*. *Journal of Oral Rehabilitation,* 24, 70–5.

Kue, R., Sohrabi, A., Nagle, D., Frondoza, C. & Hungerford, D. (1999). Enhanced proliferation and osteocalcin production by human osteoblast-like MG63 cells on silicon nitride ceramic discs. *Biomaterials,* 20, 1195–201.

Kuo, J.S., Jan, M.S., & Chiu, H.W. (2005). Mechanism of cell death induced by cationic dendrimers in RAW 264.7 murine macrophage-like cells. *Journal of Pharmacy and Pharmacology,* 47, 489–95.

Lan, S., Veiseh, M., & Zhang, M. (2005). Surface modification of silicon and gold-patterned silicon surfaces for improved biocompatibility and cell patterning selectivity. *Biosensors and Bioelectronics,* 20, 1697–708.

Lee, K.K., Bhushan, B., & Hansford, D. (2005). Nanotribological characterization of fluorpolymer thin films for biomedical micro/nanoelectromechanical system applications. *Journal of Vacuum Science & Technology: A,* 23, 804–10.

Lian, T. & Ho, R.J.Y. (2001). Trends and developments in liposome drug delivery systems. *Journal of Pharmaceutical Sciences,* 90, 667–80.

Lin, G., Pister, K.S.J., & Roos, K.P. (2000). Surface micromachined polysilicon heart cell force transducer. *Journal of Microelectromechanical Systems,* 9, 9–17.

Madou, M. (1997). Fundamentals of microfabrication (p. 471). Boca Raton, FL: CRC Press LLC.

Malik, N., Wiwattanapatapee, R., Klopsch, R., Lorenz, K., Frey, H., Weener, J.W., Meijer, E.W., Paulus, W., & Duncan, R. (2000). Dendrimers: relationship between structure and biocompatibility *in vitro*, and preliminary studies on the biodistribution of ^{125}I-labelled polyamidoamine dendrimers *in vivo*. *Journal of Controlled Release,* 65, 133–148.

Margerum, L.D., Campion, B.K., Koo, M., Shargill, N., Lai, J.-J., Marumoto, A., & Sontum, P.C. (1997). Gadolinium(III) DO3A macrocycles and polyethylene glycol coupled to dendrimers – effect of molecular weight on physical and biological properties of macromolecular magnetic resonance imaging contrast agents. *Journal of Alloys and Compounds,* 249, 185–90.

Matsumura, Y. & Maeda, H. (1986). A new concept for macromolecular therapeutics in cancer- chemotherapy – mechanism of tumoritropic accumulation of proteins and the antitumour agent SMANCS. *Cancer Research,* 46, 6387–92.

Meyer, J.U. (2002). Retina implant – a bioMEMS challenge. *Sensors and Actuators A – Physical,* 97–98, 1–9.

Moussy, F., Harrison, D.J., & Rajotte, R.V. (1994). A miniaturized Nafion-based glucose sensor – *in vitro* and *in vivo* evaluation in dogs. *International Journal of Artificial Organs,* 17, 88–94.

Nagayasu, A., Uchiyama, K., & Kiwada, H. (1999). The size of liposomes: a factor which affects their targeting efficiency to tumors and therapeutic activity of liposomal antitumor drugs. A*dvanced Drug Delivery Reviews,* 40, 75–87.

Naji, A. & Harmand, M.F. (1991). Cytocompatibility of two coating materials, amorphous alumina and silicon carbide, using human differentiated cell cultures. *Biomaterials,* 12, 690–4.

Neerman, M.F., Zhang, W., Parrish, A.R., & Simanek, E.E. (2004). *In vitro* and *in vivo* evaluation of a melamine dendrimer as a vehicle for drug delivery. *International Journal of Pharmaceutics,* 281, 129–32.

Nordsletten, L., Hogasen, A.K.M., Konttinen, Y.T., Santavirta, S., Aspenberg, P., & Aasen, A.O. (1996). Human monocytes stimulation by particles of hydroxyapatite, silicon carbide and diamond: *in vitro* studies of new prosthesis coatings. *Biomaterials,* 17, 1521–7.

Ortega, P., Bermejo, J.F., Chonco, L., de Jesus, E., de la Mata, F.J., Fernandez, G., Flores, J.C., Gomez, R., Serramia, M.J., & Munoz-Fernandez, M.A. (2006).

Novel water-soluble carbosilane dendrimers: synthesis and biocompatibility. *European Journal of Inorganic Chemistry,* 7, 1388–96.

Papra, A., Bernard, A., Juncker, D., Larsen, N.B., Michel, B., & Delamarche, E. (2001). Microfluidic networks made of poly(dimethylsiloxane), Si, and Au coated with polyethylene glycol for patterning proteins onto surfaces. *Langmuir,* 17, 4090–5.

Patri, A.K., Kukowska-Latallo, J.F., & Baker Jr., J.R. (2005). Targeted drug delivery with dendrimers: comparison of the release kinetics of covalently conjugated drug and non-covalent drug inclusion complex. *Advanced Drug Delivery Reviews,* 57, 2203–14.

Plank, C., Mechtler, K., Szoka, F.C., & Wagner, E. (1996). Activation of the complement system by synthetic DNA complexes: a potential barrier for intravenous gene delivery. *Human Gene Therapy,* 7, 1437–46.

Richards Grayson, A.C., Shawgo, R.S., Johnson, A.M., Flynn, N.T., Li, Y., Cima, M.J., & Langer, R. (2004). A bioMEMS review: MEMS technology for physiologically integrated devices. *Proceedings of the Institute of Electrical and Electronics Engineers,* 92, 6–21.

Roberts, J.C., Bhalgat, M.K., & Zera, R.T. (1996). Preliminary biological evaluation of polyamidoamine (PAMAM) Starburst™ dendrimers. *Journal of Biomedical Materials Research,* 30, 53–65.

Schatzlein, A.G., Zinselmeyer, B.H., Elouzi, A., Dufes, C., Chim, Y.T.A., Roberts, C.J., Davies, M.C., Munro, A., Gray, A.I., & Uchegbu, I.F. (2005). Preferential liver gene expression with polypropyleneimine dendrimers. *Journal of Controlled Release,* 101, 247–58.

Sharma, S., Popat, K.C., & Desai, T.A. (2002). Controlling nonspecific protein interactions in silicon biomicrosystems with nanostructured poly(ethylene glycol) films. *Langmuir,* 18, 8728–31.

Sohrabi, A., Holland, C., Kue, R., Nagle, D., Hungerford, D.S., & Frondoza, C.G. (2000). Proinflammatory cytokine expression of IL-1β and TNF-α by human osteoblast-like MG-63 cells upon exposure to silicon nitride *in vitro*. *Journal of Biomedical Materials Research,* 50, 43–9.

Stoldt, C.R. & Bright, V.M. (2006). Ultra-thin film encapsulation processes for micro-electro-mechanical devices and systems. *Journal of Applied Physics D: Applied Physics,* 39, R163–70.

Tokachichu, D.R. & Bhushan, B. (2006). Bioadhesion of polymers for bioMEMS. *Institute of Electrical and Electronics Engineers Transactions on Nanotechnology,* 5, 228–31.

Tomalia, D.A., Naylor, A.M., & Goddard, W.A. (1990). Starburst dendrimers – molecular-level control of size, shape, surface-chemistry, topology, and flexibility from atoms to macroscopic matter. *Angewandte Chemie International Edition-England,* 29, 138–175.

United States Food and Drug Administration. (1995). Required Biocompatibility Training and Toxicology Profiles for Evaluation of Medical Device. Retrieved October 20, 2006, from http://www.fda.gov/cdrh/g951.html.

Voskerician, G., Shive, M.S., Shawgo, R.S., von Recum, H., Anderson, J.M., Cima, M.J., & Langer R. Biocompatibility and biofouling of MEMS drug delivery devices. *Biomaterials,* 24, 1959–67.

Wan, H., Williams, R.L., Doherty, P.J., & Williams, D.F. (1994). Cytotoxicity evaluation of Kevlar and silicon carbide by MTT assay. *Journal of Materials Science-Materials in Medicine,* 5, 441–5.

Wan, G.J., Yang, P., Shi, X.J., Wong, M., Zhou, H.F., Huang, N., & Chu, P.K. (2005). *In vitro* investigation of hemocompatibility of hydrophilic SiN_x:H films fabricated by plasma-enhanced chemical vapor deposition. *Surface & Coatings Technology,* 200, 1945–9.

Webster, T.J., Ergun, C., Doremus, R.H., Siegel, R.W., & Bizios, R. (2000). Specific proteins mediate enhanced osteoblast adhesion on nanophase ceramics. *Journal of Biomedical Materials Research,* 51, 475–83.

Weisenberg, B.A. & Mooradian, D.L. (2002). Hemocompatibility of materials used in microelectromechanical systems: platelet adhesion and morphology *in vitro*. *Journal of Biomedical Materials Research,* 60, 283–91.

Wisniewski, N. & Reichert, M. (2000). Methods for reducing biosensor membrane biofouling. *Colloids and Surfaces B-Biointerfaces,* 18, 197–219.

Woodle, M.C. & Scaria, P. (2001). Cationic liposomes and nucleic acids. *Current Opinion in Colloid & Interface Science,* 6, 78–84.

Yang, H. & Kao, W.J. (2006). Dendrimers for pharmaceutical and biomedical applications. *Journal of Biomedical Materials Research-Polymer Edition,* 17, 3–19.

Yoo, H. & Juliano, R.L. (2000). Enhanced delivery of antisense oligonucleotides with fluorophore-conjugated PAMAM dendrimers. *Nucleic Acids Research,* 28, 4225–31.

Zhang, W., Jiang, J., Qin, C., Perez, L.M., Parrish, A.R., Safe, S.H., & Simanek, E.E. (2003). Triazine dendrimers for drug delivery: evaluation of solubilization properties, activity in cell culture, and *in vivo* toxicity of a candidate vehicle. *Supramolecular Chemistry,* 15, 607–16.

Zhu, Z., Zhang, J., & Zhu J. (2005). An overview of Si-based biosensors. *Sensor Letters,* 3, 71–88.

Ziaie, B., Baldi, A., Lei, M., Gu, Y., & Siegel, R.A. (2004). Hard and soft micromachining for bioMEMS: review of techniques and examples of applications in microfluidics and drug delivery. *Advanced Drug Delivery Reviews,* 56, 145–72.

Zimmerman, S., Fienbork, D., Flounders, A.W., & Liepmann, D. (2004). In-device enzyme immobilization: wafer-level fabrication of an integrated glucose sensor. *Sensors and Actuators B-Chemical,* 99, 163–73.

Zinselmeyer, B.H., Mackay, S.P., Schatzlein, A.G., & Uchegbu, I.F. (2002). The lower-generation polypropylenimine dendrimers are effective gene-transfer agents. *Pharmaceutical Research,* 19, 960–7.

Zuruzi, A.S., Butler, B.C., MacDonald, N.C., & Safinya, C.R. (2006). Nanostructured TiO_2 thin films as porous cellular interfaces. *Nanotechnology,* 17, 531–5.